Article:
Zhang, Y, Colombera, L orcid.org/0000-0001-9116-1800, Mountney, NP et al. (7 more authors) (2021) Sedimentation of open-framework gravels in alluvial-fan settings: Quaternary Poplar Fan, northwest China. Marine and Petroleum Geology. 105376. p. 105376. ISSN 0264-8172

https://doi.org/10.1016/j.marpetgeo.2021.105376

Sedimentation of open-framework gravels in alluvial-fan settings: Quaternary Poplar Fan, northwest China

Yue Zhang[1], Luca Colombera[2], Nigel P. Mountney[2], Chonglong Gao[3], Youliang Ji[1*], Heng Wu[4], Wei Du[5], Dawei Liu[6], Donglai Bai[1], Wanda Song[7]

1. State Key Laboratory of Petroleum Resource and Prospecting and College of Geosciences, China University of Petroleum (Beijing), Beijing 102249, China;

2. Fluvial, Eolian & Shallow-Marine Research Group, School of Earth and Environment, University of Leeds, Leeds, LS2 9JT, UK;

3. Institute of Unconventional Oil and Gas, Northeast Petroleum University "Fault Deformation, Sealing and Fluid Migration" Science and Technology Innovation Team in Colleges and Universities of Heilongjiang, Daqing, Heilongjiang 163318, China;

4. College of Information Engineering, Hebei GEO University, Shijiazhuang, Hebei 050000, China;

5. CNOOC International Limited, Beijing 100028, China;

6. Petroleum Exploration and Production Research Institute of SINOPEC, Beijing 102206, China;

7. SINOPEC Geophysical Corporation Shengli Branch, Dongying, Shandong 257100, China.

Abstract

Open-framework gravels (OFGs) form common lithofacies of alluvial fans. However, inferences of their mechanisms of transport and deposition, and of controls on their distribution in alluvial-fan successions, remain difficult, limiting our ability to interpret the environmental significance of such deposits and to predict their distributions in ancient successions. From an applied standpoint, such predictions are important in the development of hydrocarbon reservoirs and remediation of aquifers hosted in alluvial-fan strata. To elucidate our understanding of formative conditions of different types of OFGs, a study has been undertaken on the Quaternary Poplar Fan, in the endorheic Heshituoluogai Basin, China.

Based on observations from outcrops and trenches on the Poplar Fan, eight different types of OFGs are identified: these lithofacies types account for 7% of the total deposits of the fan. During high flow stages, OFGs are deposited in association with supercritical sheet-like flow (type 1), unconfined streamflow (type 2), and flow in groundwater-fed channels (type 3). During low flow

* Corresponding author.

E-mail address: jiyouliang2017@126.com (Youliang Ji).

stages, OFGs are associated with trough cross-stratification (type 4) and sigmoidal cross-stratification (type 5); these types occur over the entire fan. At the fan margins, OFGs are associated with gulleys (type 6), especially at the distal fan toe. Other OFG types are associated with bank collapse (type 7) or intercalated with aeolian deposits (type 8). A model is proposed to account for the distribution of different types of OFGs across the fan, wherein types 1, 2 and 4 seen in the medial fan are dominant. This provides a framework for the identification, prediction and correlation of OGFs in subsurface alluvial-fan successions.

Keywords: open-framework gravels, conglomerate, alluvial fan, facies model, heterogeneity, openwork.

1. Introduction

Alluvial-fan deposits are an important component of many continental sedimentary basin fills, especially of those fronting mountain ranges (Blissenbach, 1954; Ventra and Clarke, 2018). Alluvial-fan successions are highly variable and can exhibit complex sedimentary architectures recording a variety of formative processes (DeCelles et al. 1991; Shukla, 2009). Alluvial fans are notably characterized by a broad range of facies types. Among these, some alluvial-fan successions comprise open-framework gravels (OFGs) that are notably poor in sandy sediment or muddy matrix and are typically well-sorted. These gravel lithofacies can form in different sedimentary sub-environments and can be preserved as deposits that vary with regard to bedding and sedimentary structures (North and Warwick, 2007; Wang et al, 2007; De Haas et al., 2015a; Zhang, C.M. et al., 2020). The recognition and prediction of these facies in subsurface alluvial successions acting as oil reservoirs or aquifers is important because of their marked influence on fluid flow in relation to their high pore connectivity and permeability (Zhang 1985; Wang et al, 2007; Wu et al, 2012). Particularly in programs of oil production by water injection, the permeability contrasts caused by OFGs can determine the presence of thief zones that can cause early water breakthrough. Hence, production strategies, such as plugging, need to be implemented to efficiently exploit the resources they may contain (Ferreira et al., 2010; Gershenzon et al., 2015a; Burbery et al, 2017; Gong et al, 2019).

Different mechanisms of origin and distribution of OFGs are documented, and these vary as a function of different environmental conditions. For example, OFGs are known to occur at the front, top and sides of tongue-shaped bodies deposited by debris flows (Major, 1997; Parsons et al., 2001; Hürlimann et al., 2003; Johnson et al.,

2012; De Haas et al., 2015b; Kim et al., 2021). OFGs are seen to occur in planar-tabular stratified couplets mantling the surface of sheetflood-dominated alluvial fans (Ballance, 1984; Blair, 1999), and as basal accumulations in channel fills of fluvial fans (Jo et al., 1997; Trendell et al., 2013; Clarke 2015; Miall 2014; Jolivet et al., 2015; Gao et al., 2018). However, the genesis of OFGs in stream-flow-dominated alluvial-fan systems subject to high-magnitude, episodic floods is not fully accounted for by existing depositional models. For this type of systems, the origins, character and distribution of OFGs need further examination and interpretation. Such analysis can contribute to our understanding of the processes of alluvial-fan deposition, which in turn can guide predictions of the presence and characteristics of openwork gravels or conglomerates in subsurface successions, where their occurrence and distribution may have applied significance (Burbery et al., 2017; Kang et al., 2017; Gong et al., 2019).

The aim of this study is to quantitatively characterize the distribution and origin of open-framework gravels in stream-flow-dominated alluvial-fan successions that record deposition by both streamflow and mass-flow processes, associated with both high and low flow stages. Specific research objectives are: (i) to undertake a sedimentological investigation of the Quaternary Poplar alluvial fan, NW China; (ii) to undertake detailed description and particle-size analysis of the OFGs of the Poplar Fan; (iii) to map the distribution of different types of OFGs across the fan surface and to relate such deposits to other associated lithofacies and architectural elements; and (iv) to develop a generic facies model to account for the occurrence of OFGs across fan sectors, in relation to mechanisms of fan construction and growth.

2. Geological setting

The Quaternary Poplar Fan is located in the northern part of the Heshituoluogai Basin, NW China (Fig.1-A). The development of this basin was initiated through thrust-nappe tectonics involving the northern Xiemisitai Fault and southern Darbut Fault during the Triassic. The internal structural conditions of the Heshituoluogai Basin are complex: several thrust faults are present at both the basin margin and within its interior. Of these, the Xiemisitai Mountain piedmont fault and the Darbut fault in the northern and southern parts of the basin, respectively, played an important role in controlling basin development by tectonic loading during the Triassic (Sun, 2015; Gao et al., 2018). Although many of the internal faults within the basin are mostly covered by Quaternary and recent sediments and have no surface expression, some faults break to the surface such that their traces - some expressed as fault-zone

arrays - are evident (Fig. 1-A).

The Poplar Fan has been constructed adjacent to the active boundary fault of the Xiemisitai Mountain and is fed by a drainage catchment with an area of ~2,000 km^2 and an average slope of 2.1°. Sediment-laden floods from this catchment reach the fan surface via a feeder valley. The catchment bedrock mostly consists of Devonian to Permian volcanic and pyroclastic rocks, whereas the piedmont zone is locally underlain by Cenozoic and Jurassic sedimentary rocks (Qu et al., 2008). The Quaternary Poplar Fan is 31 km long, has a maximum width of 37 km and a surface area of 730 km^2. Its age spans from Early Pleistocene to Holocene (<2.58 Ma), as determined from lithostratigraphic relationships and analysis of magnetic fabric documented from outcrops located at the fan apex and in the proximal fan area (Du et al., 2013; Ai and Ji, 2015). The Quaternary sediments are mainly unconsolidated piedmont alluvial deposits, dominantly gravels, composed of different lithologies. Relatively fine-grained (φ>-1) deposits represent only 6% of the fan sediments. The Poplar Fan is currently traversed by a single river, which is locally entrenched into the fan surface. At the fan head, the valley of the Poplar River is 28 to 40 m deep; the depth of valley incision decreases downstream, and the streambed becomes unconfined at the fan toe. Presently the Poplar river flows in a U-shaped valley that extends along the entire fan length (Fig.1-B).

In response to neotectonic activity, a series of small-scale secondary alluvial-fan systems have developed in the downthrown blocks along the traces of intra-fan thrust faults in the eastern part of the fan. In contrast, the western part does not reveal any distinguishable fault traces at the surface (Fig.1-B). The apex of the eastern Poplar Fan is at an elevation of 900 m a.s.l. due to uplift through reverse faulting, whereas the highest point of the western Poplar Fan is at an elevation of 820 m. The distal sector of the fan ranges in elevation from 490 m a.s.l. in the southeast to 640 m a.s.l. in the northwest. The thickness of the accumulated fan succession varies from ~200 to 400 m, based on calculation of the elevation difference from the proximal to the distal fan. At its distal toe, the fan transitions to an alluvial plain. The slope of the eastern part of the fan varies considerably in its proximal region, where the surface is as steep as 3°; the slope from the medial fan to its fringe remains approximately constant at 0.7°. In contrast, the slope of the western part of the fan, which is less influenced by faulting, is near-constant at 0.6°.

The climate of the Heshituoluogai Basin is arid to semiarid. The Poplar River is highly seasonal. A 46-year (1962 to 2007) record of monthly average water discharge data exists for a hydrological station in the upper reach of the Poplar River, near the

fan apex (Ran et al., 2010) (Fig. 2). From 1962 to 2007, the maximum runoff occurred between April and July, reflecting the combined contribution of snow melting and precipitation (Table 1). The greatest precipitation is recorded in late July and August, but in these months the water runoff tends to decrease, chiefly because of transmission losses due to evaporation, leading to a downstream decrease in river size towards the piedmont plains.

During the season of peak discharge, the Poplar River can flood due to rainstorm, snow melt, or a combination of the two (Lin et al., 1996; Rhodes et al., 1996; Zhao et al., 2009) (Fig. 3). Individual flood events occur over periods of several hours to several tens of hours. The flow rate changes significantly over the course of a flood. Paroxysmal geomorphic change of the fan surface takes place during floods that typically last a few days or less (Li, 2008; Ran et al., 2010). The episodic floods tend to be characterized by high discharge rates and sediment concentrations; these floods tend to accumulate sheet-like deposits. As a flood recedes and the discharge and sediment concentration of the flood flow decrease, channelization of the fan surface occurs.

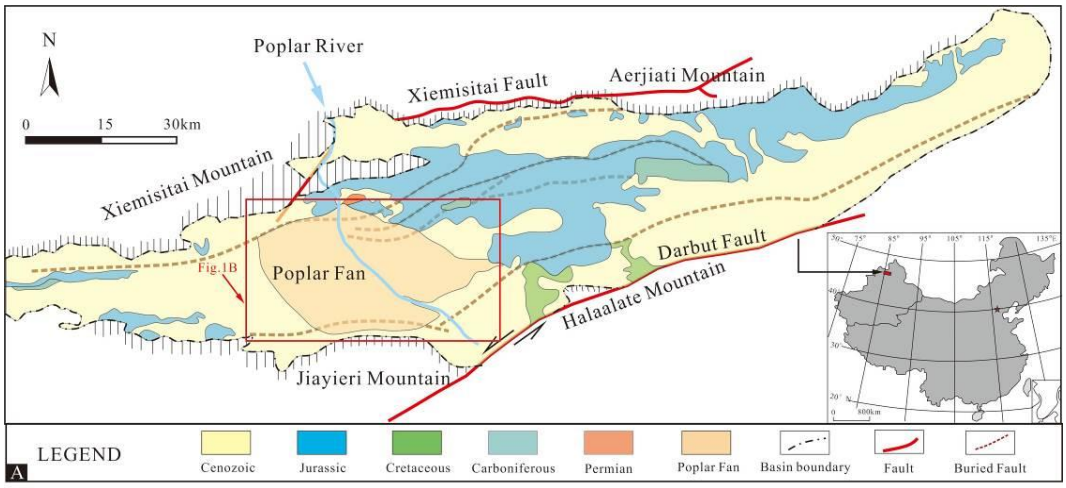

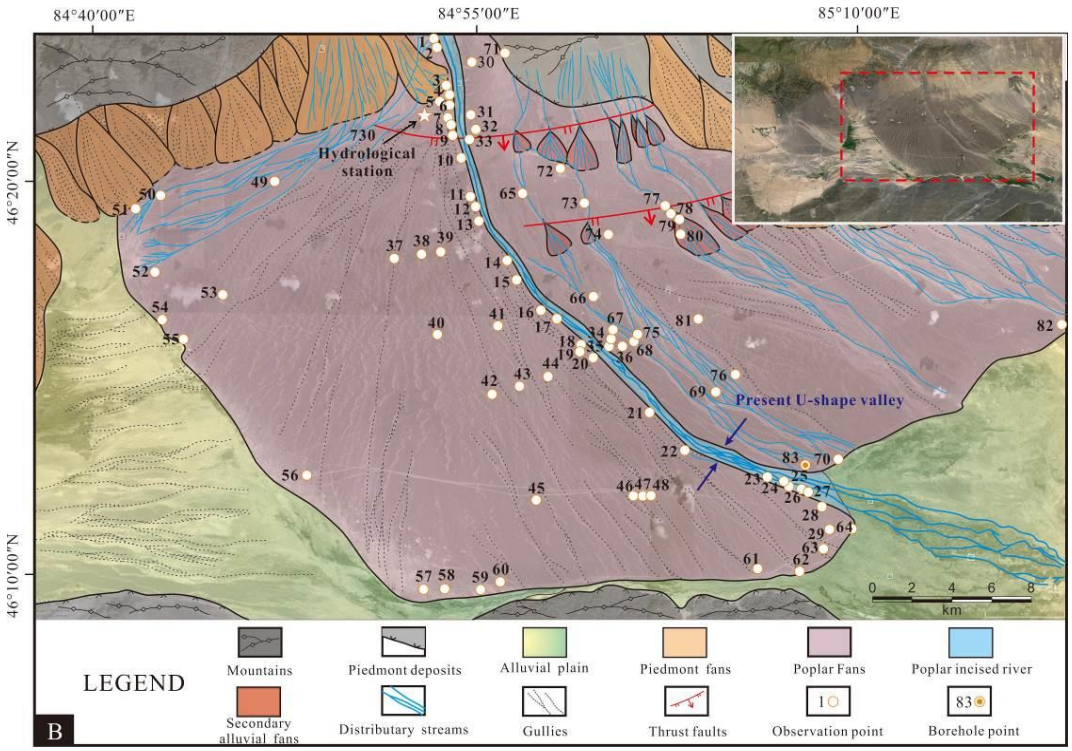

Fig.1 (A). Map showing lithological units and major thrust fault planes surrounding and within the basin and the modern Poplar River and Poplar Fan (modified from Qu et al., 2008; Ma et al., 2015; Shen et al., 2015). Locations where observations are made are labelled. (B). Google Earth™ satellite image of the study area with interpreted overlay.

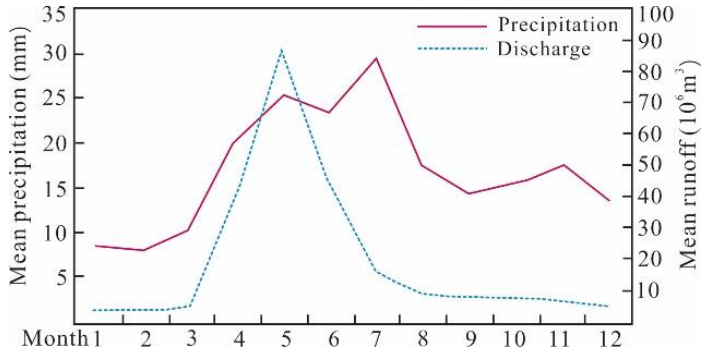

Fig. 2 Monthly mean precipitation and average monthly runoff recorded at the 730 Hydrological Station over a 46-year interval (1962 to 2007) (modified from Ran et al., 2010).

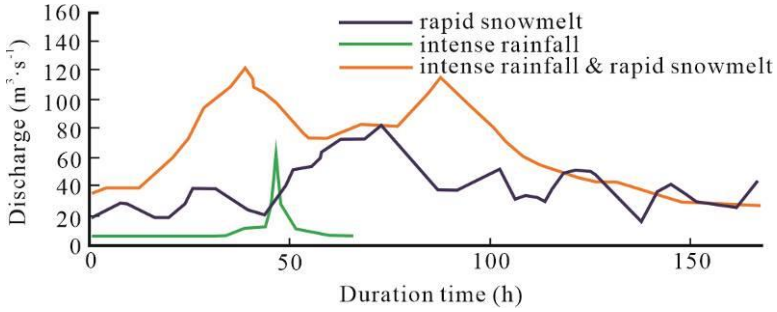

Fig. 3 Hydrographs of three single flood events recorded at 730 Hydrological Station (Fig.1-B), which were

respectively triggered by intense rainfall (19 July 1996), by rapid snowmelt (6 May 1995), and by the combined effect of intense rainfall and rapid snowmelt (2 May 1988) (modified from Ran et al., 2010).

Table 1 Seasonal runoffs of Poplar River recorded in 730 Hydrological Station

Annual Runoff (10^8 m^3)	Percentage of seasonal relative to annual water discharge (%)				month of minimum discharge	month of maximum discharge	Four consecutive months of maximum water discharge	
	March -May	June-August	September-November	December -February			months	Annual percentage (%)
2.450	55.9	28.5	9.9	5.9	February	May	Apr-Jul	77.6

3. Data and Methods

In total, 83 exposures on the Poplar Fan, including natural outcrops and trenches, were logged and analysed to study the origin, character and distribution of open-framework gravels in the fan deposits (Fig. 1B). The studied locations are mainly distributed along the western wall of the incised valley of the Poplar River. These study locations include outcrops oriented down-fan, quarry faces oriented along depositional strike and eight dug trenches. Twenty-six individual sedimentary logs with a cumulative total length of 168.8 m were measured. The logs record the occurrence of OFGs and other facies types with a vertical resolution of 10 cm. Additionally, data on maximum clast diameter and clast composition were recorded. At all studied locations, units of OFGs were characterized in terms of their horizontal extent, thickness, and proportion (as a ratio of cumulative thickness of OFGs and total thickness of measured section observed in outcrop).

Sieve analyses were undertaken to determine the detailed grain-size distributions of 39 samples of OFGs. The hydrodynamic conditions of sedimentation were inferred through graphical analysis of grain-size distributions by calculating statistical moments (SK, KG, σ1) and by plotting Coarsest-Median (C-M) diagrams, whereby C and M are respectively the 1^{st} and 50^{th} (median) centiles of frequency distributions. The shape of the cumulative distribution function (CDF) was used to estimate the hydrodynamic conditions of the formative water flow (cf. Visher, 1965, 1969; Folk, 1966; Sahu, 1964; Doeglas, 1968). Grain-size statistics (e.g. σ1, SK_I, K_G) were interpreted in terms of their geological significance (cf. McManus, 1988; Blot and Pye, 2001).

4. Results

4.1 Processes, geomorphology and sediments of the Poplar Fan

The Quaternary Poplar Fan is dominated by episodic floods. Landforms and deposits associated with flood and interflood processes are summarized here.

High-energy episodic floods are characterized by sediment-laden flows that emanate from the mountain catchment. The flows cover all or most of the fan surface and most occur as sheet-like flows (Jo et al., 1997). Sediments in the catchment area are eroded through undercutting of slope deposits and are entrained by catastrophic floods, resulting in hyperconcentrated flood flows (cf. Blair and McPherson, 2009). During the low flow stage, seasonal braided streams migrate across the river valley; these misfit streams scour and rework sediments that were deposited during the preceding high flow stage. Sediment deposition associated with these processes is recorded by eleven principal lithofacies types, which encompass the majority of the deposits seen on the fan surface; these facies types are summarized in Table 2.

In the proximal fan, the fan-head trench was formed by erosion of flood deposits, which in part takes place during the high flow stage itself (cf. Hooke 1967) (Fig. 4A). Disorganized gravels with beds of outsized clasts (G1) dominate in this sector (Fig. 6A); direct observations record that these represent the product of hyperconcentrated flows close to the threshold between plastic and turbulent flows (Pierson and Scott, 1985; Harvey, 1999). In the medial fan sector, hyperconcentrated floods tend to transform into supercritical sheet-like flows (Gao et al., 2020), with bedload transport resulting in the accumulation of stratified gravels with rhythmically interbedded sands (Blair, 1999, 2000). In this sector, typical lithofacies include planar-horizontal bedded gravels (G2) and sands (S1), which are laterally continuous for tens to hundreds of metres (Fig. 6B, F). In the medial to distal fan, supercritical sheet-like flows tend to transition to streamflow in braided channels flowing around mid-channel barforms. Planar-horizontal bedded gravels (G2) and sands (S1) are not developed here; instead, gravels with low-angle cross-stratification (G3) are prevalent in this sector (Fig. 6C). In the most distal fan-fringe region, the streamflow is conveyed by numerous narrow and shallow channels, which diminish in size to a point where they locally terminate into an ephemeral wetland, directly beyond the fan toe. The deposits of this sector are dominated by cross-bedded gravels (G4), rippled sands (S4) and silty muds (M1) (Fig. 6E, I, J).

During the low flow stage (Fig. 4B), streamflow over the Quaternary Poplar Fan occurs in low-sinuosity, locally braided, channels. In the proximal fan, the river flows

through a single-thread channel (Fig. 5A). Here, the gravel clasts forming the riverbed have a diameter of more than 30 cm (Fig. 5B). In the medial sector of the fan, the channel-belt widens (Fig. 5C), and channel bifurcations develop around channel bars (Fig. 5D). Here, the sediment is dominated by gravels with a diameter of 10-20 cm. Trough cross-bedded conglomerate (G4) (Fig. 6D) occurs in 0.5 m to 1 m-thick cosets, which internally contain cross beds that are 5 to 10 cm thick sets. These cross bedded units are formed in laterally mobile braided river channels (Fig.4). In the medial fan, the river flows in a wide valley, with a sinuosity index of 1.22 (Fig. 5F). Here, it develops a large number of gravel bars with varied forms. Sparse vegetation, consisting mostly of grasses and shrubs grows on the surface of the bars. The gravels are finer, with clasts having a diameter of 5 to 15 cm. At the distal end of the fan, both sides of the valley are flanked by aeolian sand dunes or depressions (Fig. 5E). In this region, the river channel has a sinuosity of 1.36 and consists of anabranching channel threads yielding an average bifurcation index of 5.0 (Fig. 5H), with well-developed vegetation, including well-established trees and shrubs. The sediments are mainly fine gravels and sands. Planar-horizontal bedding in sands (S1) (Fig. 6F) indicates dominant bedload deposition under conditions of upper-flow regime (Miall, 1996; Jo et al., 1997). Cross-bedded sands (S2) and ripple cross-laminated sands (S4) with silty muds (M1) occur in the upper portions of channel successions (Parker, 1983; Miall, 1996). Across the fan surface, occasional rainstorms and groundwater can flow within gulleys that are ~1 m wide and have limited extent downfan (typically 3 to 6 km); these tend to be intermittently active in the summer, when the local water-table rises due to groundwater infiltration (Fig. 5G).

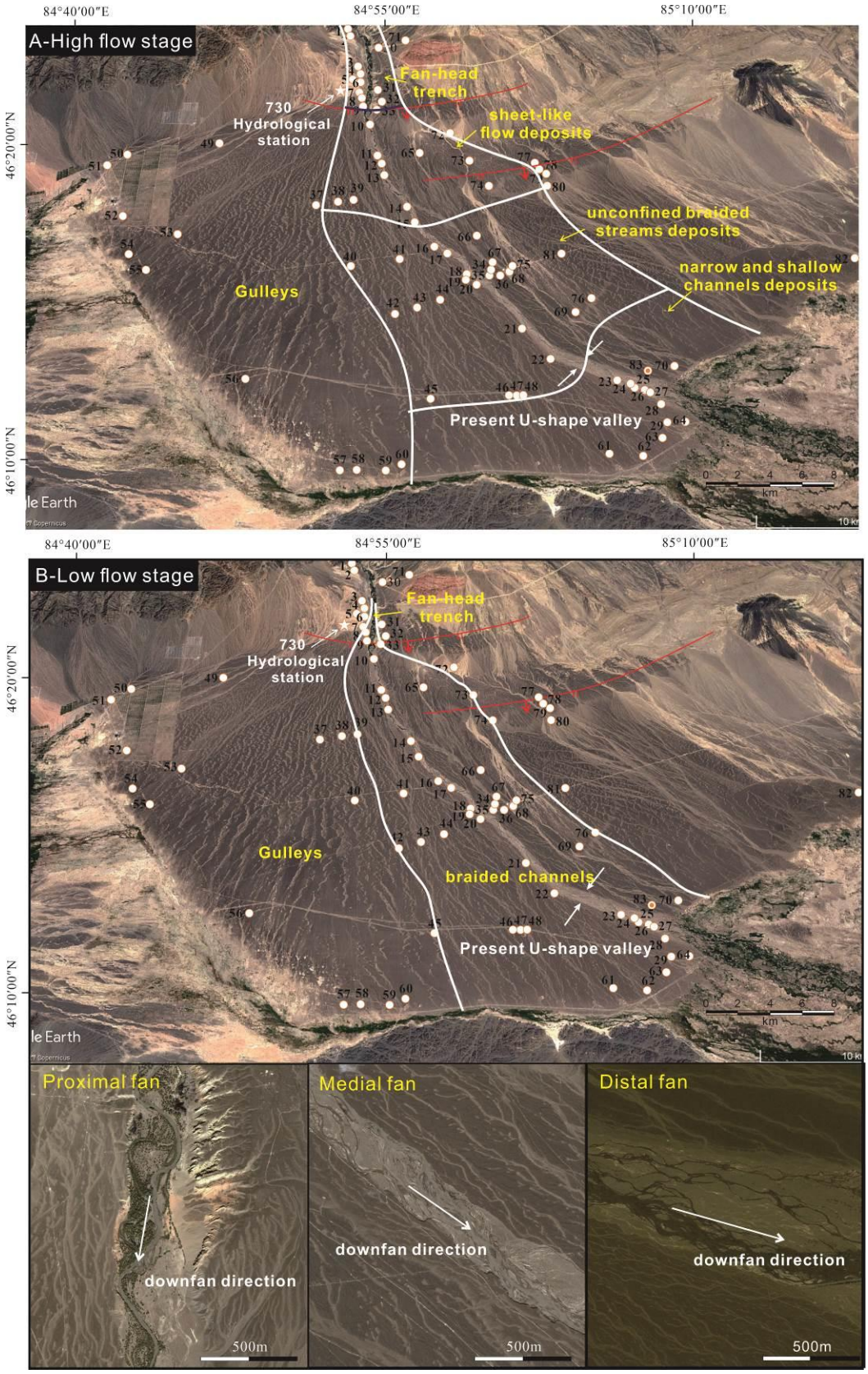

Fig. 4 Google Earth™ satellite imagery of the Poplar Fan. (A) Extent of areas of the Poplar Fan subject to different dominant processes during the high flow stage. (B) Domains of the Poplar Fan associated with the low flow stage.

Fig. 5 Geomorphological features of the Poplar Fan. (A) Main channel in the proximal fan at observation point 1. (B) Deposits of channel bed at observation point 9. (C) Wider channel at observation point 10. (D) Bifurcating channels with mid-channel bar at observation point 12. (E) Ephemeral wetland at observation point 69. (F) Bifurcating channels and mid-channel bars at observation point 20. (G) Gulleys at observation point 76. (H) Narrow channels at observation point 22.

Table 2 Summary of the main lithofacies types identified on the Poplar Fan and their interpreted origin. The types of open-framework gravels (OFG types) observed in each facies type are also reported.

Lithofacies	Sedimentary textures and structures	Spatial distribution	Interpretation	OFG types
Massive gravels (G1)	Disorganized boulder to cobble gravels, with 2-10 cm gravel diameter, gravels matrix and common outsized clasts up to 0.8 m; local gravel imbrication; no discernible grading	catchment feeder channel to fan-head trench	High-energy floods carrying clasts of variable sizes (2-80 cm), through a combination of traction, buoyancy, and dispersive pressure (Pierson and Scott, 1985; DeCelles et al., 1991; Blair, 1999)	Type 4 and type 7 OFGs
Planar-horizontal bedded gravels (G2)	Rhythmic couplets of boulder and cobble conglomerates, clast-supported, with crude planar horizontal stratification; laterally continuous for tens to hundreds of metres	proximal to medial fan	Deposition by supercritical sheet-like flows (Fr=1.4-2.8) (Blair, 2000; Blair and McPherson, 2009)	Type 1 OFGs
Gravels with low-angle inclined cross bedding (G3)	Massive, clast-supported cobble to sandy pebble conglomerates with low-angle inclined (5°-10°) cross-stratification; locally indistinct cross-stratification; laterally continuous for tens to hundreds of metres	medial fan	Bedload sheets or traction carpets associated with high flow velocity (Reid and Frostick, 1987; Jo et al., 1997)	Type 2 OFGs
Gravels with trough cross bedding (G4)	Clast-supported, crudely stratified cobble to pebble conglomerate, with wedge-shaped/lenticular geometries or tabular bedded; high-angle (10°-20°) cross bedding, with 0.5-1 m thick sets made of laminae that are 5-10 cm thick	channelized deposits	Subcritical bedload deposition by streamflows (Froude number<1) (Miall, 1977; Shukla, 2009)	Type 4 OFGs and type 5 OFGs

Gravel clusters (G5)	Clast-supported clusters of massive gravels, with 1-2 cm modal gravel diameter, 5-10 cm thickness of a single set, fining-upward to S4	channelized deposits in distal fan, reworked and abandoned or inactive fan sectors	Bedload transport under lower flow regime, within channels or gulleys (De Haas et al., 2015a; Antronico et al., 2015)	Type 3 OFGs and Type 6 OFGs
Planar-horizontal bedded sands (S1)	Locally pebbly, medium to coarse sands, with planar horizontal stratification	channelized deposits	Upper flow regime bedload deposition (Fr>1) (Jo et al., 1997; Cain and Mountney, 2009)	None
Trough cross-bedded sands (S2)	Medium to coarse sands with wedge-shaped/lenticular geometries or tabular bedded, erosional bases, and high-angle (10°-20°) trough cross bedding, with 0.5-1 m thick sets containing laminae that are on average 2 cm thick	channelized deposits	Bedload, lower-flow regimes, vertical and lateral accretions of dunes or unit bars in restricted channels (Siegenthaler and Huggenberger, 1993; Jo et al., 1997)	None
Planar pin-stripe laminated sands (S3)	Sharply bounded, medium to coarse sands, with planar pin-stripe laminations; small-scale low-angle (3 to 7°) foresets toed by tangential transitions into planar bed can be identified, laterally discontinuous, 5 to 10 cm thick lenticular or tabular units	aeolian sand dunes or sand sheets	Wind deposition on the fan surface (Blair, 1999; Blair and McPherson, 2009; Mountney, 2012; Gao et al; 2020)	None
Ripple cross-laminated sands (S4)	Locally silty fine sands, 10 to 80 cm thick, forming irregular to lenticular units with erosional bases; typically arranged in fining-upward trend	distal fan	Bedload transport under lower flow regime, ripples within restricted channels (Fr<0.4) (Blair and McPherson, 2009; Shukla, 2009)	None
Silty muds (M1)	Non-stratified (muddy) silty and (silty) muds, massive	distal fan	Suspended load fallout deposition in a standing-water environment (Trendell et al., 2013)	None

Fig.6 Selected photos of lithofacies of the Poplar Fan. (A) Massive gravels with locally developed gravel imbrication; G1. (B) Planar-horizontal bedded gravels; G2. (C) Gravels with low-angle cross bedding; G3. (D) Gravels with trough cross bedding; G4. (E) Gravel clusters; G5. (F) Planar-horizontal bedded sands; S1. (G) Trough cross-bedded sands; S2. (H) Planar pin-stripe laminated sands; S3. (I) Ripple cross-laminated sands; S4. (J) Silty muds; M1.

4.2 Deposits of open-framework gravels

Overall, the observed open-framework gravels are characterized by a lack, or limited proportion (less than 15%), of sand or fines (φ>-1) between the gravel clasts (Allan and Frostick, 1999; Zhang et al., 2020a). Herein, OFGs are considered separately from the above-mentioned lithofacies. As defined in this work, the same facies can contain more than one OFG type; in addition, the same OFG type can be present in more than one facies type. Open-framework gravels account for ~7% of the entire alluvial-fan sedimentary succession. The proportion of OFGs is particularly limited in proximal fan areas (<1%), increases to a maximum in the medial fan (15%), and decreases again towards the fan fringe, where OFGs only occur sporadically. In the deposits of the Poplar Fan, eight types of OFGs are identified based on detailed analysis of sedimentary fabric, sedimentary structures and bedding style. These types are observed or interpreted to result from different genetic mechanisms, and reflect categorization based on inferred or observed depositional conditions and sub-environments.

Type 1 - open-framework gravels associated with supercritical sheet-like flow

Description

Type 1 OFGs occur as part of sheet-like flow deposits in the proximal to medial fan region. These OFGs occur in the basalmost part of bodies of facies G2. They occur as layers of cobble gravels with gravel clast diameters ranging from 2 cm to 8 cm in beds that are on average 0.3 m thick. The gravels are mostly sub-rounded to rounded and [a(t) b(i)] imbricated. The upper part of beds consists mostly of small pebbles, capping an overall fining-upward arrangement. Planar beds of this deposit commonly occur amalgamated, forming composite successions up to 0.5 m thick. The lateral extent of units of this OFG type can be several tens to hundreds of metres (Fig.7-A).

Interpretation

The couplets defining the rhythmic interbedding of lithofacies G2 are interpreted as a record of the repetitive formation and collapse of supercritical standing waves within a sheet-like flow (Blair and McPherson, 2009; Cao et al., 2017; Tan et al., 2018), indicating that these OFGs may form the coarse portion of deposits of supercritical sheet-like flow. Supercritical sheet-like flows with high Froude numbers (Fr = 1.4 ~ 2) (Blair, 1999, 2009) are characteristic of catastrophic flood events (Pierson and Scott, 1985; Sohn, 1997; Blair and McPherson, 2009; Antronico et al., 2015; Banham and Mountney, 2013). These OFGs are interpreted to be associated with high turbulence

accompanying washout, which causes coarse-fraction sorting. The fining-upward trend indicates the rapid abatement of local turbulence; the intermittent suspended load rapidly falls out of the flow and is transported as traction load, accumulating as a laminated couplet consisting of a fine unit in sharp contact upon the coarse bed (Blair, 1999, 2009). The coarsest portion of the unit was deposited as bedload, whereas the suspended and quasi-suspended load was likely carried further downflow (Blair, 1999, 2000).

Type 2 - open-framework gravels associated with unconfined subcritical streamflows

Description

Type 2 OFGs are locally seen at the base of units of facies G3 in the medial fan. They take the form of stacked massive, tabular or lenticular conglomerate bodies. They are characterized by faint trough cross-stratification. They exhibit irregular erosional bases defined by trough surfaces that are typically inclined at a low-angle (5° to 10°). Gravel clast diameters range from 5 to 10 cm and occur in beds that are on average 10 cm thick. Pebbles are mostly sub-rounded to rounded, more so than for the Type 1 OFGs. Deposits above the basal scour surface usually fine upward within individual beds. Individual depositional units of this OFG overlap and are locally truncated by the erosional bases of neighbouring units. These OFGs have lateral extents of several tens of metres (Fig.7-B).

Interpretation

Units of this OFG type represent the basalmost parts of unconfined-streamflow successions. Slight fluctuations in flow energy during the high flow stage could have resulted in the formation of faint cross-stratification (Blair and McPherson, 2009). Wide, shallow unconfined streamflows result from the waning of supercritical sheet-like flows, and can be unsteady and non-uniform subcritical (Fr<1) turbulent flows (Jo et al., 1997; Shukla, 2009; Clarke et al., 2010; Waters et al., 2010). Specifically, the abundant trough infills and lenticular features are interpreted as the product of deposition under conditions of lower flow regime. The low-angle cross-stratification of G3 and parts of the individual depositional units of these OFGs are truncated by low-relief erosional bases of neighbouring units; these are interpreted to have been sculpted by rapidly shifting narrow and shallow channel forms (Allen, 1981; Jo et al., 1997). Type 2 OFGs are interpreted to have been transported as bedload sheets or as traction carpets in subcritical turbulent streamfloods, which are usually characterized by high sediment concentrations (Shukla, 2009; North and

Davidson, 2012). The fining-upward sequence records the effects of waning flow.

Type 3 - open-framework gravels associated with groundwater-fed channels

Description

Type 3 OFGs occur as parts of narrow and groundwater-fed shallow channels in the distal fan. They occur as part of facies G5, and are characterized by thin layers of irregular geometry and non-erosional bases. This OFG type exhibits rounded gravel clasts with diameters ranging from 0.2 to 1 cm forming beds with thickness of ca. 10 cm. Units of these OFGs are 1 to 5 m wide; they span the width of the groundwater-fed channels in which they are seen. Beds of these OFGs display a fining-upward trend, and transition vertically into silty muds (Fig.7-C). They are encased in a facies association containing the finest deposits of the Poplar Fan and consisting of unstratified muddy siltstone or silty mudstone of lithofacies M1.

Interpretation

The vertical reduction of grain sizes is interpreted to reflect temporally decreasing flow energy. Type 3 OFGs with irregular geometry or forming clusters indicate that they could be sourced from thin lags of coarse clasts through winnowing, or from coarse sediments derived from bank collapse (Gao et al., 2020). Their relationship with the fine-grained distal-fan facies association indicates that Type 3 OFGs reflect a high-energy environment in a wetland setting of the distal fan. The broad range of widths of units of Type 3 OFGs may reflect variability in water discharge, determining variability in the size of groundwater-fed channels.

Type 4 - open-framework gravels associated with trough cross-stratification

Description

Type 4 OFGs occur as parts of braided-channel deposits present across the entire fan. They occur at the base of units of facies G4. Units of this OFG contain notably less sandy and fine-grained matrix than other OFG types. The gravels are imbricated with their long axis planar to flow, and the intermediate axis transverse to flow. They exhibit scour surfaces at the bottom of the braided channels. The mean gravel-clast diameter varies from 5 to 30 cm. In the proximal fan, this OFG type is expressed as lenticular coarse-gravel bodies associated with C1, in which gravel clasts range from 10 to 30 cm and are well rounded (Fig.7-D-1, 2). The lateral extent of these deposits is ~10 m, equivalent to that of the hosting channels. The mean thickness of cross-sets is ca. 0.5 m. In the medial fan, units of this OFG type contain clasts with diameters of 5 to 10 cm. The OFG is present in sets of trough cross-bedding (sets with thickness of

ca. 0.3 - 0.5 m). Cross beds with rhythmic intercalation of coarse- and fine-grained sediment occur as lateral-accretion packages (with beds inclined at 10° to 20°) (Fig. 7-D-3, 4).

Interpretation

The presence of trough cross-bedding indicates bedload deposition. Trough cross-bedding is widely reported as the most common structure in the central and lower parts of alluvial and fluvial channel fills (e.g., Cuevas-Gozalo and Martinius, 1993; Colombera and Mountney, 2019). Lateral accretion suggests that braided channel threads experienced lateral thalweg shifts (Fig. 7-D-3, 4). Type 4 OFGs at the proximal fan were deposited in channels whose water depth enhanced the formation of larger cross-set, and where relatively high flow velocities facilitated the transport of coarser grain-sizes. The range in cross-set thickness of type 4 OFGs suggests the coexistence of palaeochannels with different discharges (Miall, 1977; Shukla, 2009).

Type 5 - open-framework gravels associated with sigmoidal cross-stratification

Description

Type 5 OFGs occur as parts of braided channel deposits across the entire fan. They are present in channel fills, and are more common in the proximal fan region (up to 15% of the deposit volume) than in downstream fan region (< 1% of deposit volume). These deposits are intimately associated with units of facies G4. They are observed at the head and along the sides of presently active mid-channel bars. They contain gravel clasts ranging in diameter from 2 to 10 cm. Their lateral extent ranges from 1 to 5 m, which reflects the scale of channel bars. In profile, these OFG units form lenticular bodies that internally exhibit sigmoidal or wedge-shaped accretion geometries in cross-section (Allen, 1983a, b; Lunt et al., 2004; Lunt and Bridge, 2007) (Fig.7-E). Each set of sigmoidal cross-stratification is between 4 to 10 cm thick and displays some normal grading; cross-strata dip at angles of 7 to 15° and have well-defined boundaries. They form 0.2 to 1 m-thick lenticular units with erosional concave-up bases.

Interpretation

Sigmoidal or wedge-shaped cross-stratification can be produced by barform accretion in braided rivers (Steel and Thompson, 1983; DeCelles et al., 1991). Variations in grainsize reflect the hydrodynamics of streamflows around the bars. The bars accrete across pools when secondary currents wane (Cuevas Gozalo and Martinius, 1993; Chen et al., 2017; Goswami et al., 2018). Where OFGs occur near the top of compound bar deposits, they are commonly a product of the migration of coarse

bar-head unit bars. Coarse material is carried onto the upstream end of the nucleus of the exposed flat (Lunt et al., 2004). Type 5 OFGs record deposition at the head and along both sides of the bars. Because the bars occur as part of braided channel deposits, Type 5 OFGs almost always occur in close association with Type 4 OFGs.

Type 6 - open-framework gravels associated with gulleys

Description

Type 6 OFGs occur as parts of gulley deposits across reworked and abandoned or inactive fan sectors. This type commonly occurs as thin interlayers within the fine-grained deposits at the fringe of the fan. Gravel clast diameters range from 1 to 10 cm. Units of this OFG type have a mean thickness of 0.5 m. They occur at the base of G5 and take the form of isolated lenticular beds associated with sandy deposits. Their average width is ca. 1 m; they are therefore narrower than Type 4 OFGs (Fig.7-F).

Interpretation

These deposits are interpreted to be product of reworking by ephemeral surficial flows due to rainwater convergence on the alluvial fan (Antronico et al., 2015; De Haas et al., 2015a). In the distal fan where the gulleys hosting these deposits are seen, flows may be accumulative (spatially non-uniform), faster than in upstream areas, and with high transport capacity (Gao, 2018). These flows may winnow finer sediment leaving behind clean openwork gravels. The association of isolated lenticular beds of Type 6 OFGs with fine-grained deposits, together with their erosional bases and mature texture, suggest that deposition took place in the form of bedload deposition alternating with suspension fallout.

Type 7 - open-framework gravels associated with bank collapse

Description

Type 7 OFGs are seen in the fan-head trench and valley in the proximal to medial fan. Open-framework gravels associated with bank or valley-wall collapses are locally identified in longitudinal profiles along the middle and downstream reaches of the valley walls. Units of this OFG type are mainly composed of scattered gravels with poor sorting and chaotic fabric. Gravel clast diameters range from boulder to fine gravel at different locations. These deposits form fan-shaped accumulations or irregular aprons, in which coarser clasts accumulate farther away from the collapsed margin (Fig.7-G).

Interpretation

Type 7 OFGs form as the product of gravitational bank collapses, as observed on the surface of the fan along valley walls. In outcrop, the abundance of coarse cobbles and boulders in lower portions indicates their transportation by rolling. Spatial distributions in clast size record gravitational runout associated with particle momentum.

Type 8 - open-framework gravels associated with aeolian activity

Description

Type 8 OFGs occur throughout the fan. Units of this OFG type tend to occur most commonly as accumulations with apparently chaotic structure, located around desert shrubs. These OFGs were deposited at the back of accumulations of planar pin-stripe laminated sands (S3), which represent the aeolian deposits of coppice dunes around desert shrubs. Gravel clasts vary in diameter from 5 to 30 cm across the different locations (Fig.7-H).

Interpretation

These OFGs are formed by winnowing by wind activity. The fine-grained material on the surface of the original deposit is entrained and transported away by the wind (Al-Farraj et al., 2000; Pullen et al., 2018), leaving behind residual gravels that form Type 8 OFGs.

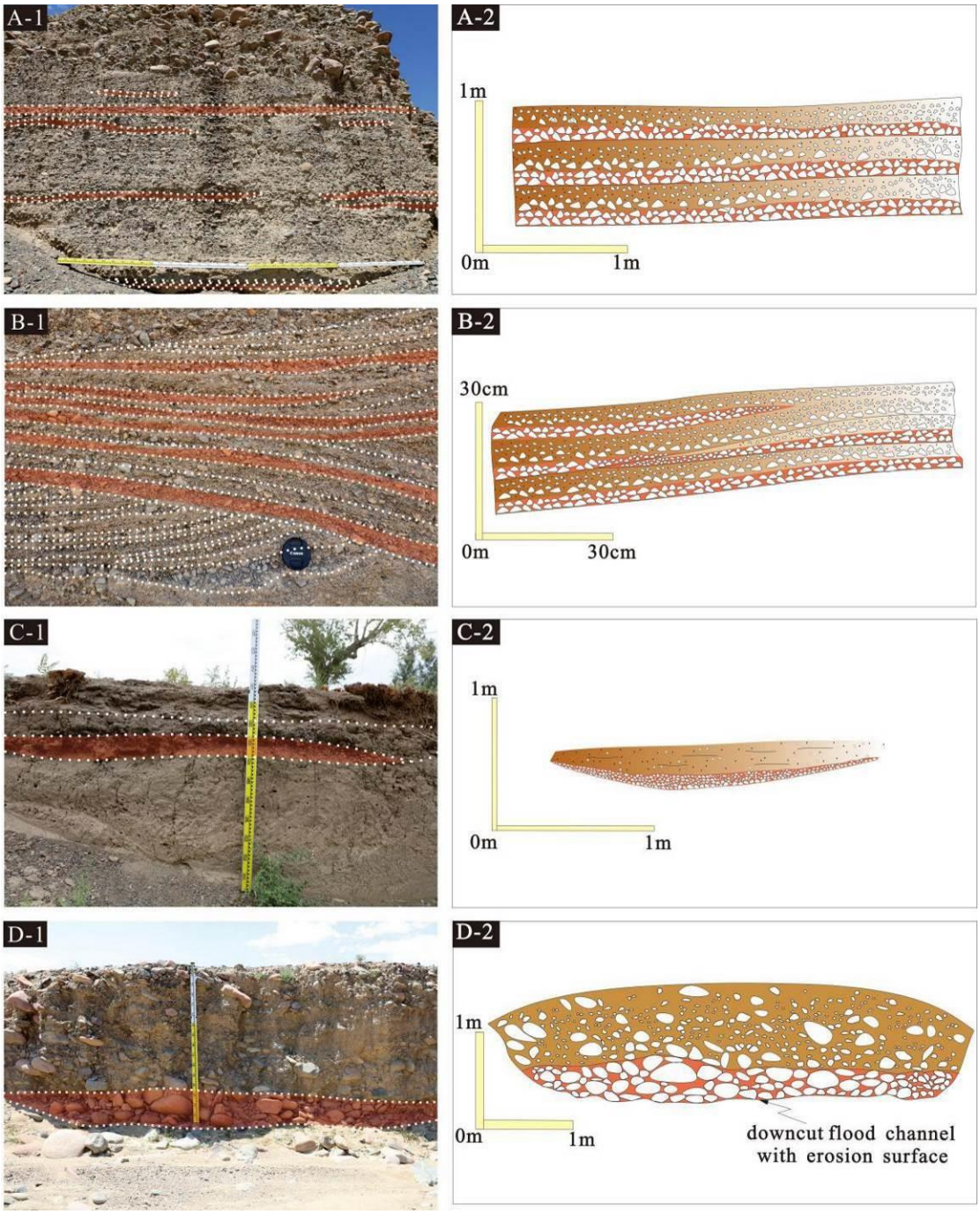

Fig.7 Examples of open-framework gravels of the Poplar Fan, marked by red transparent overlays in outcrop photos. (A) Type 1 OFGs associated with supercritical sheet-like flow. (B) Type 2 OFGs associated with braided streams. (C) Type 3 OFGs associated with local surface runoffs. (D) Type 4 OFGs associated with restricted channel bases. (E) Type 5 OFGs associated with channel bars. (F) Type 6 OFGs associated with gulleys. (G) Type 7 OFGs associated with bank collapse. (H) Type 8 OFGs associated with aeolian winnowing.

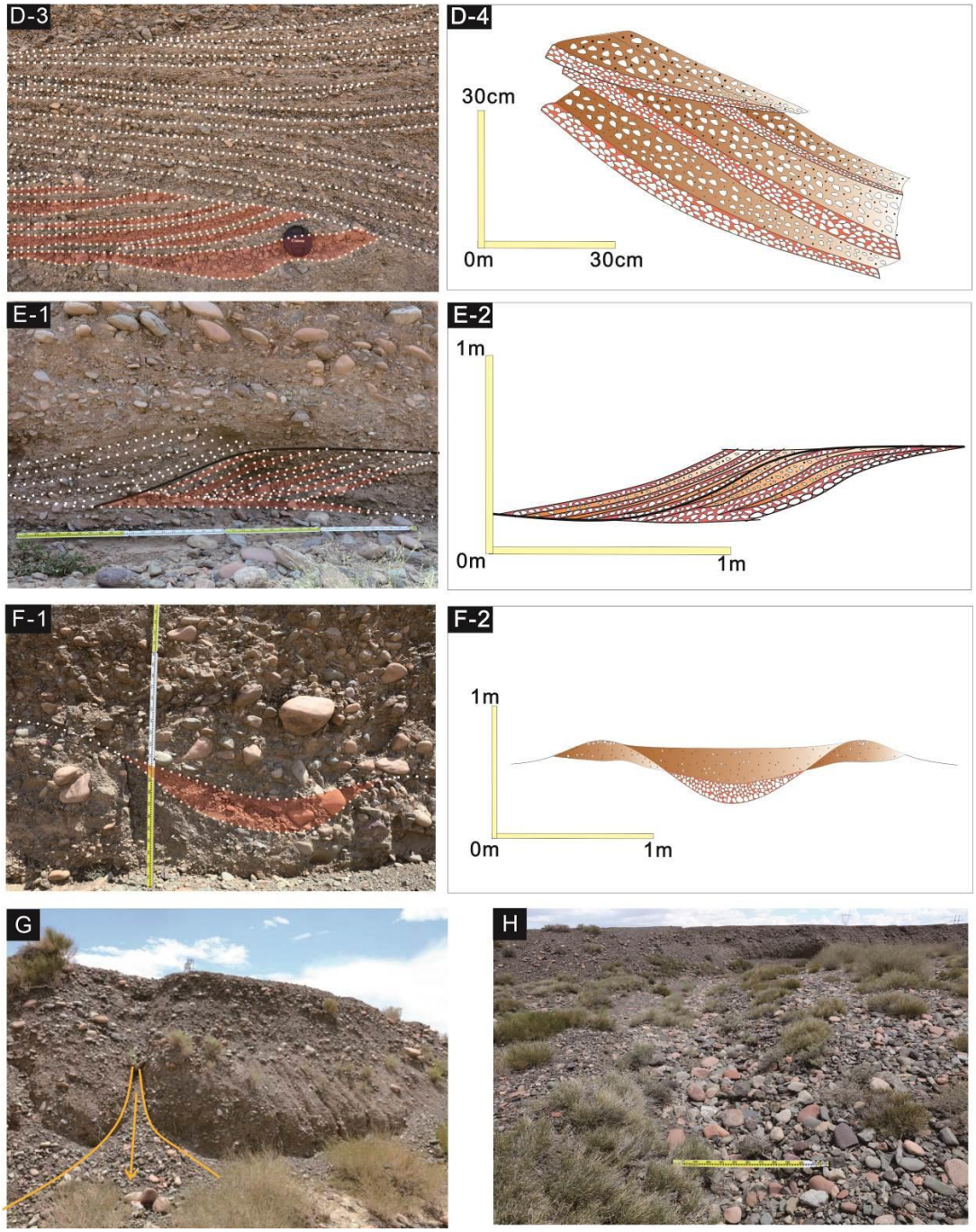

4.3 Grain-size characteristics of open-framework gravels

Grain-size variations

The gravel-clast diameter of the main types of open-framework gravels is analysed at 19 locations along the valley. The maximum and average grain sizes of different types of open-framework gravels are measured at each location.

Grain-size data record an overall reduction in OFG gravel clast size from the proximal fan to the fringe, but in a fluctuating manner (Fig. 8). This trend is consistent with variations in the origin of deposits on the fan, in relation to how OFG deposition is

related to flow processes. The OFGs mainly consist of cobble to boulder gravels, for which the maximum diameter of the major axis is 3 to 30 cm and the average diameter of the major axis is 2 to 9 cm.

In deposits related to the high flow stage, the largest-clast diameter of Type 1 OFGs takes maximum values between 6 to 10 cm, and average values between 1.3 and 5.0 cm. Type 2 OFGs exhibit the maximum values of the largest clast diameter between 7 and 9 cm, whereas average values are 2.0 and 4.5 cm. Type 3 OFGs exhibit maximum values of the longest gravel clast axis between 8 to 11 cm, which is the largest grain sizes recorded in the distal fan. The occurrence of these deposits in distal-fan settings is a likely record of major flood events with exceptionally large discharges and sediment loads.

In deposits related to the low flow stage, the grain size of type 4 OFGs sharply decreases from the proximal to the distal fan (Fig. 8). In the proximal fan region, the maximum values in gravel clast major axis are between 10 to 30 cm; mean values in major axis are between 5 to 8 cm (Fig.7-D-1, 2). In the medial to distal fan, the maximum value in gravel clast major axis is 5 to 9 cm; the average value in major clast axis is 1.5 to 3.0 cm (Fig.7-D-3, 4). Type 4 OFGs represent the most energetic hydrodynamic conditions of the low flow stage. The decreasing grain-size trend indicates a downstream reduction in sediment transport capacity of channelized flows.

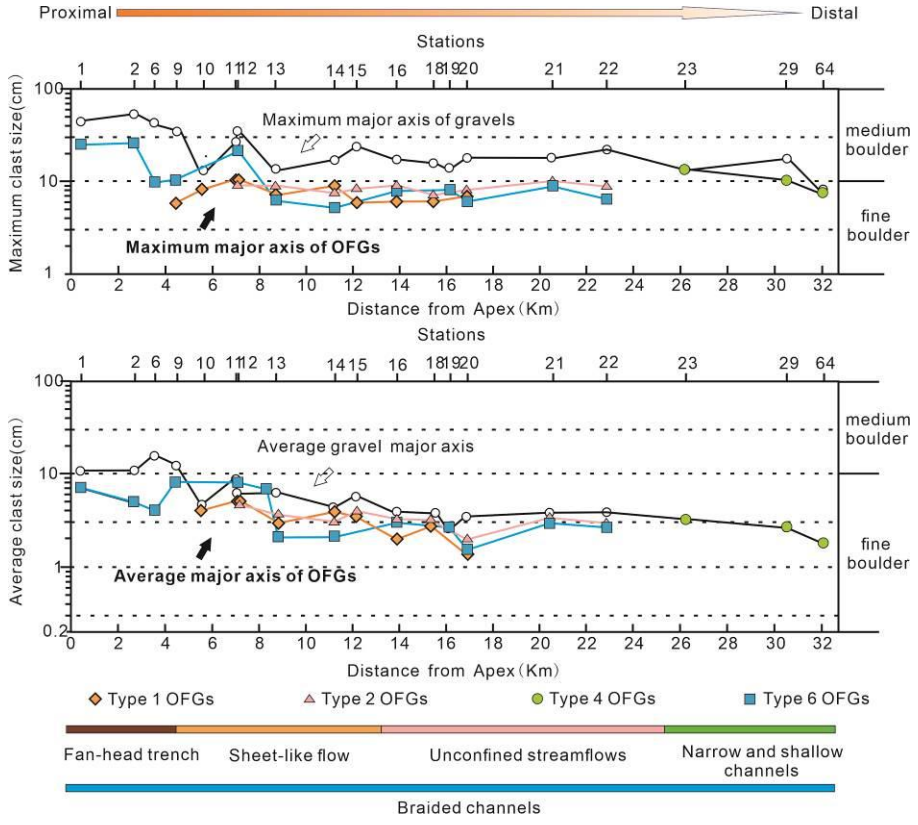

Fig.8 Downslope variations in maximum and average clast diameters of the open-framework gravels across the entire Poplar Fan. The overall maximum and average clast diameters decrease from the proximal to the distal fan.

Grain-size characteristics of open-framework gravels

Grain-size cumulative distribution functions can be employed to infer depositional mechanisms (Visher, 1965, 1969; Folk, 1966; Sahu, 1964; Doeglas, 1968). Grain size parameters can be plotted to aid interpretation of formative hydrodynamic conditions. In particular, the C-M diagram (where C indicates the 1st centile, i.e. an approximation of the maximum grain size, and M indicates the 50th centile, i.e. the median grain size) can be employed to help establish relationships between sediment texture and depositional processes (Passega, 1957). Type 1, 2, 4 and 6 OFGs are the most common on the fan. The samples of these four types have obvious differences in grain-size characteristics.

Type 1 OFGs have an average gravel content of 90% (range 88 to 99 wt%), an average sand content of 10%, and no appreciable proportion of mud. The CDFs of these deposits exhibit multiple breaks in slope and are weakly convex-upward, whereby the boundaries of each population are not marked by obvious inflection points (Fig. 9-A-1); this may represent a characteristic of gravity flows (Glaister and Nelson, 1974). However, the proportion of sand (suspension population) is limited to no more than 10% and the imbricated gravels (Fig.6-A) indicate that most of the sediments were transported by bedload; yet a portion might have possibly been transported as suspended load. The frequency distribution is mainly characterized by a single mode, with a sharp peak, between -5 ~ -3.5 Φ (Fig. 9-A-2). The kurtosis (KG) is 0.99 to 1.97 (Fig. 10-A) and the standard deviation (σ1) is 1.02 to 1.95 (Fig. 10-B); the sorting of Type 1 OFGs is the poorest of these four types. On the C-M diagram the data of Type 1 OFGs are approximately parallel to the baseline of C = M (Fig. 11). This indicates that the supercritical sheet-like flow has the characteristic of non-cohesive debris-flow to turbulent flow. Some samples are close to the baseline of C = M (Fig. 11), that is, the 1st centile is close to the median, indicating good sorting of these samples of Type 1 OFGs (Passega, 1957, 1964).

Type 2 OFGs have an average gravel content of 97% (range: 96 to 99 wt%), and 3% sand on average. The CDF is convex-upward and shows multiple breaks in slope, whereby the saltation population of most samples is divided into two linear segments (Fig. 9-B-1). Sands (suspension population) make up less than 3% of the deposit, indicating that the Type 2 OFGs are dominantly transported by bedload (Reid and Frostick, 1987; Jo et al., 1997). However, the convex-upward and segmented shape of the curve is similar to that of Type 1 OFGs, which is inferred to record non-uniform

turbulent subcritical streamflood flows, albeit less energetic than supercritical sheet-like flows. The frequency distribution is characterized by a sharp single mode between -5 ~ -3.5Φ (Fig. 9-B-2). The kurtosis (KG) is 0.84 to 1.74 (Fig. 7-A) and the standard deviation is 0.86 to 1.65 (Fig. 10-B); thus, these deposits are better sorted than Type 1 OFGs. In the C-M diagram, the corresponding data plot around the median line, almost planar to the baseline of C = M. This indicates that the unconfined streamflows were deposited under conditions of relatively high energy, about Fr<1 (Reid and Frostick, 1987; Blair and McPherson, 2009). Some samples are close to the baseline of C = M, which indicates good sorting (Fig. 11).

Type 4 OFGs show a prominent pebble mode (95% average content of gravels; range: 90 to 99 wt%) and 5% average content of sand. Three or four slope breaks in the CDF are seen: the traction population (whose boundary is marked by the first slope break) account for about 50%-80%. This indicates that the transport of type 4 is dominated by bedload. The saltation population makes up about 20%-50% of the volume, and is divided into two or three linear segments. There is little or no suspension population (Fig. 9-C-1), as is common for streambed conditions. A sharp single mode is seen between -4.5 ~ -1.6 Φ (Fig. 9-C-2). The kurtosis (KG) is 0.84 to 1.37 (Fig. 10-A) and the standard deviation is 0.93 to 1.94 (Fig. 10-B); the sorting is better than Type 2 OFGs. The C-M diagram portrays data that do not plot parallel to the baseline of C = M; this feature is characteristic of sediment transport by traction. The C-M pattern of type 4 OFGs is divided into two segments: OP and PQ (Fig.11), which corresponds with coarse sediments deposited by tractive currents (Passega, 1957, 1964). The C-M pattern of Type 4 OFGs represents moderately well-sorted sediments transported almost entirely by bedload along channels beds.

Type 6 OFGs have 98% average gravel content (range: 94 to 99 wt%) and 2% average sand content. The samples are characterized by two to three well-defined log-normal segment breaks (Fig. 9-D-1), similar to what indicated by Visher (1969) as typical of most modern river sands. These observations can be considered indicative of deposition by flows transporting sediment by traction. A single mode that is sharper than that of other types is seen between -5.5 ~ -2 Φ (Fig. 9-D-2). The kurtosis (KG) is 0.81 to 1.35 (Fig.10-A) and the standard deviation is 0.77 to 1.75 (Fig. 10-B): the sorting is better than that of types 1, 2 and 4. The C-M pattern of Type 6 OFGs is in the NO segment, which is all composed of traction population (Fig. 11). This indicates that they likely accumulated at the base of channels, to form beds composed of particles corresponding to those concentrated at the bottom of the suspension (Passega, 1957, 1964).

A-1)

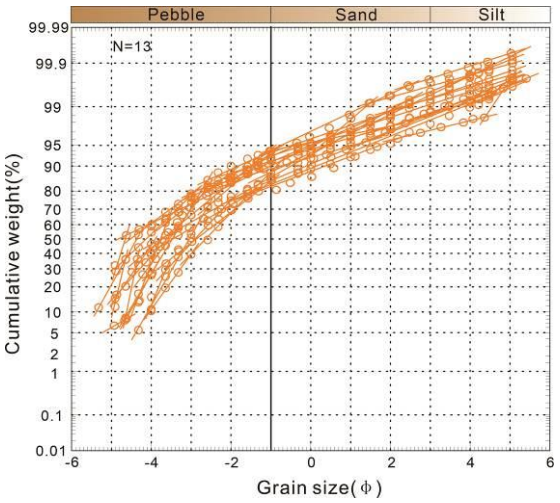

A-2)

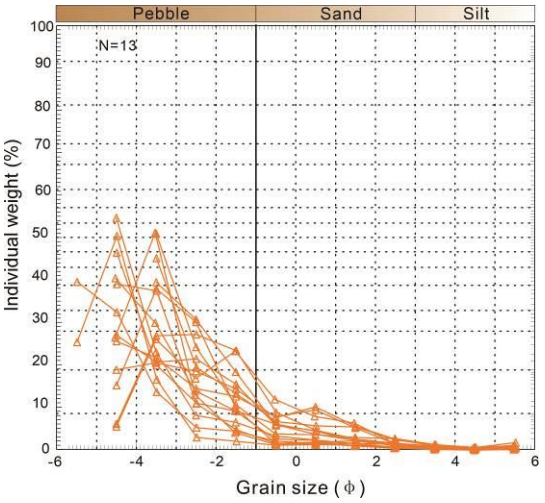

B-1)

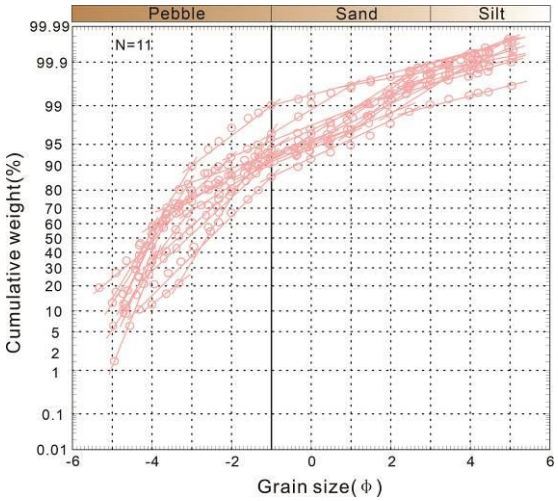

B-2)

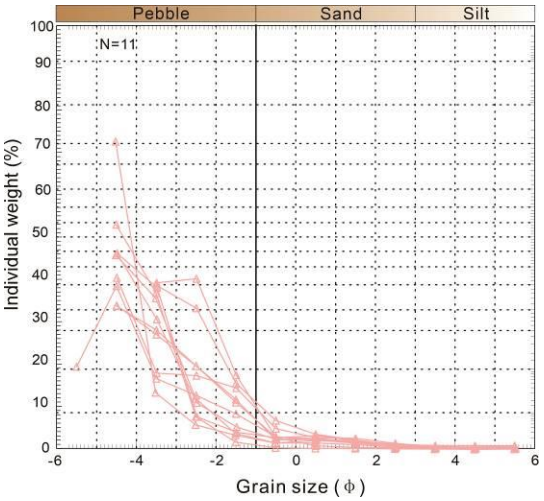

C-1)

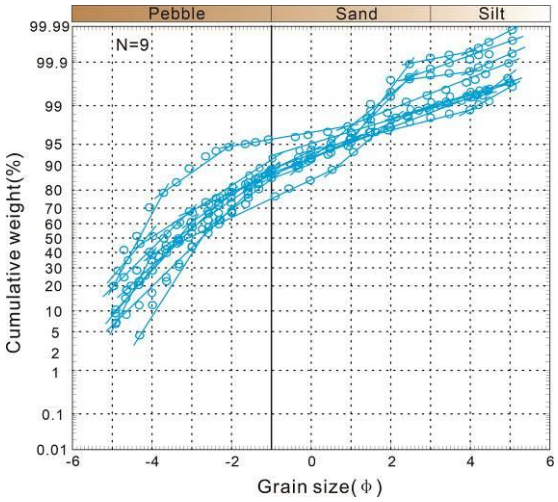

C-2)

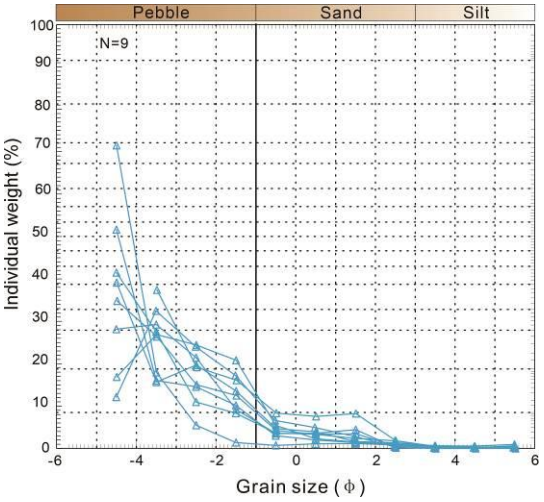

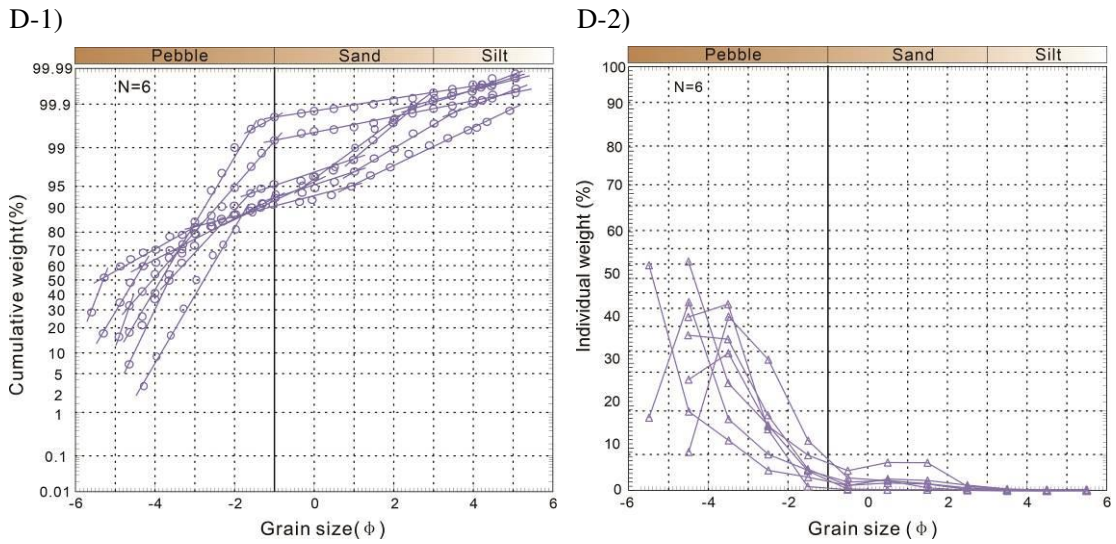

Fig.9 Cumulative distribution curves and grain-size distribution curves of different types of open-framework gravels of the Poplar Fan. (A-1) Cumulative probability curve of samples from type 1 OFGs. (A-2) Grain-size distribution of samples from type 1 OFGs. (B-1) Cumulative probability curve of samples from type 2 OFGs. (A-2) Grain-size distribution of samples from type 2 OFGs. (C-1) Cumulative probability curve of samples from type 4 OFGs. (A-2) Grain-size distribution of samples from type 4 OFGs. (D-1) Cumulative probability curve of samples from type 6 OFGs. (A-2) Grain-size distribution of samples from type 6 OFGs.

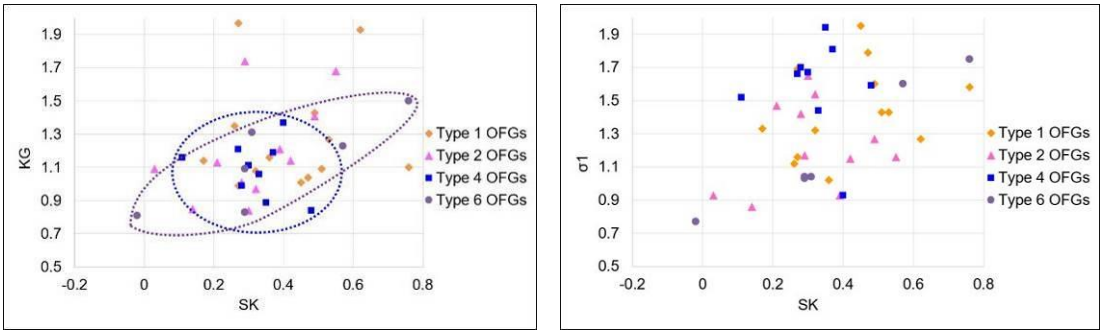

Fig.10-(A) Statistical moments skewness (SK) and kurtosis (KG) of different types of open-framework gravels of the Poplar Fan. (B) Statistical moments skewness (SK) and standard deviation (σ_1) of different types of open-framework gravels of the Poplar Fan.

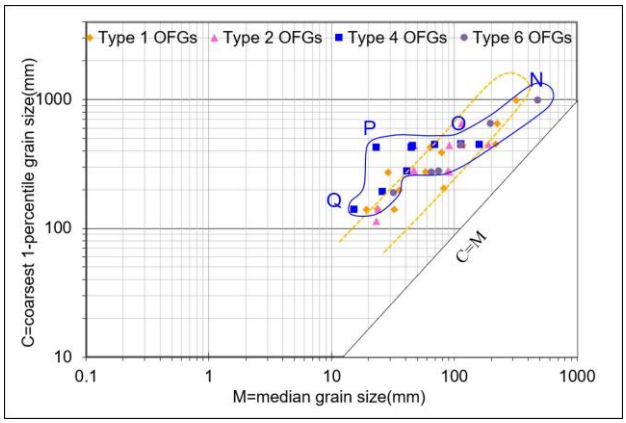

Fig.11 C-M diagram of different types of open-framework gravels of the Poplar Fan.

4.4 Distribution of open-framework gravels

Based on statistics of the lateral extent, bed thickness and proportion of units of different types of OFGs along the downfan depositional profile, different facies zones for OFGs are established.

In the high flow stage, Type 1 OFGs develop in sheet-like flow deposits and unconfined braided-stream deposits in the medial fan. Examples of such depositional units extend along strike for more than 5 m, and in some cases even tens to >100 m (cf. Blair, 2000); however single beds are thin, on average ca. 10 cm (Fig.12). The proportion of Type 1 OFGs is highest in the sheet-like flow deposits of the proximal fan (ca. 20%), and smallest in the unconfined braided streams deposits of the medial fan (ca. 10%). Type 2 OFGs occur in sheet-like flow deposits and unconfined braided streams deposits. Such units have lateral extents that are ca. 4 m on average, and mean bed thickness of ca. 10 cm. The proportion of Type 2 OFGs is highest in unconfined braided streams deposits, where it represents 14% of the overall accumulation. Type 3 OFGs develop in the narrow and shallow channels of the distal fan, where their lateral extent along strike ranges from 1 m to 5 m, and is only rarely more, i.e., it corresponds with the width of the channels in which they occur; their beds are ca. 10 cm thick on average. The proportion of Type 3 OFGs varies from 3% to nearly 30%. The trends of increasing length, thickness and proportion towards the distal fan may be related to the confluence of narrow and shallow channels and the influence of Hortonian overland flow.

In the low flow stage, Type 4 OFGs develop in braided channels across the whole fan. Such units extend along strike for more than 5 m at the fan apex, where their extent reflects the width of the streambed and the lack of bifurcations. Towards the proximal fan, the lateral extension of these units decreases to ca. 1 to 3 m. The bed thickness is also largest at the proximal fan (over ca. 50 cm) and decreases downstream to ca. 20

cm. The proportion of Type 4 OFGs is also highest (20%) in the incised valley at the fan apex, and tends to decrease downfan to a minimum of 4% (Fig.12).

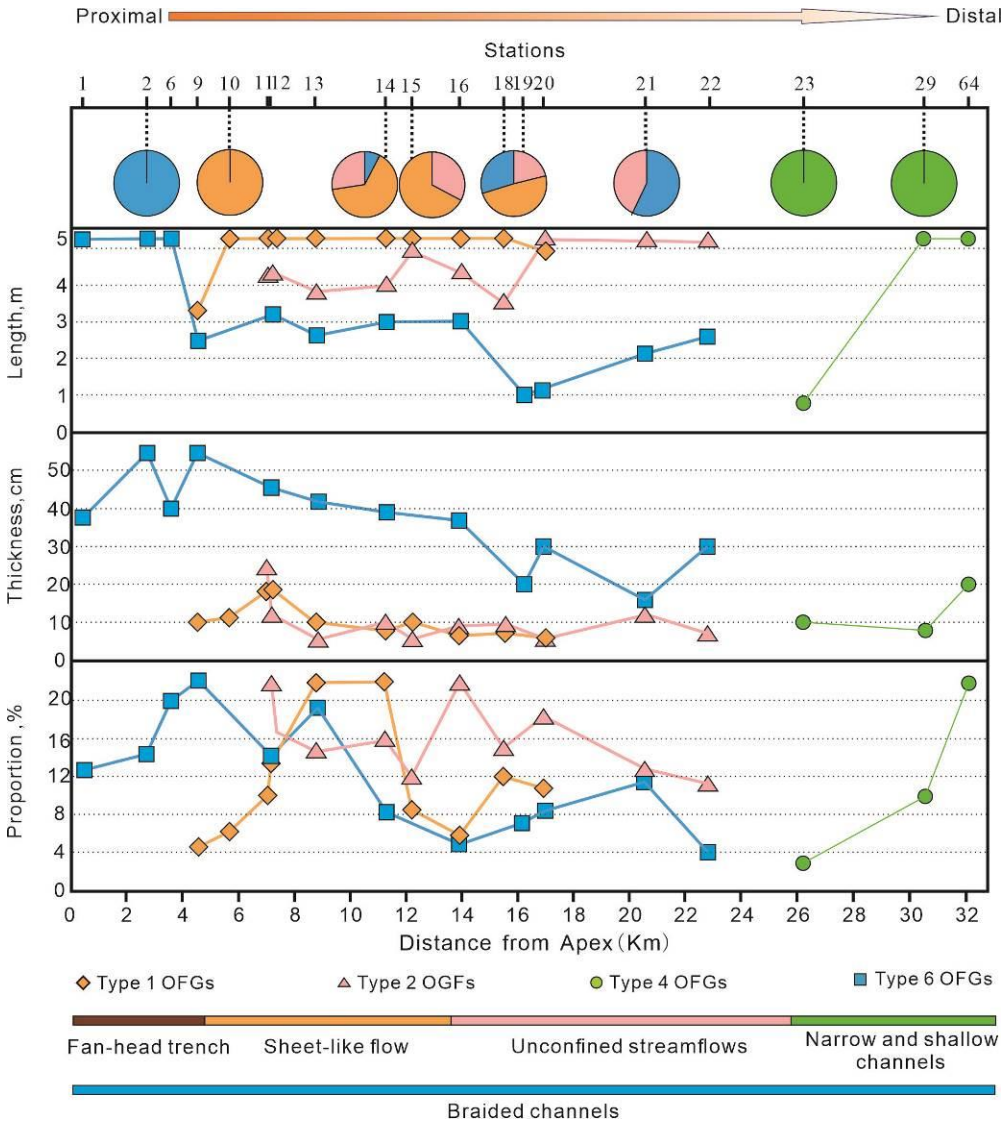

Fig. 12 Downslope variations in the lateral extent along outcrop exposures, average thickness and proportion of different types of OFGs throughout the fan.

Sediments of high and low flow stages tend to be interbedded; therefore, different types of OFGs can be seen to vary in proportion along the depositional profile and along strike. Near the fan apex, no OFG types of high flow stage are observed. Only Type 4 OFGs of low flow stage origin are observed, whose lateral extension is related to the width of the main channel (Fig. 13-A, B). In addition, some isolated lenticular units of Type 4 OFGs occur at the proximal fan, infilling scours eroded in the deposits of the high flow stage (Fig. 13-B). In the proximal to medial fan, the Type 1 OFGs associated with G2 facies are dominant. Also, a subordinate amount of Type 2 OFGs associated with G3 facies are seen interbedded with type 1 OFGs (Fig.13-C). The

lateral boundary of these OFGs can be indistinct, which indicates that their deposition was concomitant, possibly in relation to flow transformation from supercritical sheet-like flow to unconfined streamflows (Jo et al., 1997; Shukla, 2009). A limited proportion of Type 4 OFGs with cross bedding show erosional contact with underlying Type 2 OFGs (Fig. 13-C). Towards the medial fan, the Type 1 OFGs gradually disappear. Only some Type 2 OFGs of high flow stage are preserved. At the medial fan, Type 4 OFGs tend to rest directly on Type 2 OFGs via an erosional surface (Fig. 13-D) and show frequent internal unconformities caused by amalgamation of the deposits of adjacent channels. At the fringe of the fan, rare Type 3 OFGs occur locally on the streambed of narrow channels (Fig. 13-E). Type 3 OFGs are associated with lithofacies S1 and M1, where these narrow channels locally terminate into an ephemeral wetland at the distal fan. On both sides of the fan, Type 6 OFGs are interbedded with G4 facies in the deposits of gulleys traversing the distal fan (Fig. 13-F).

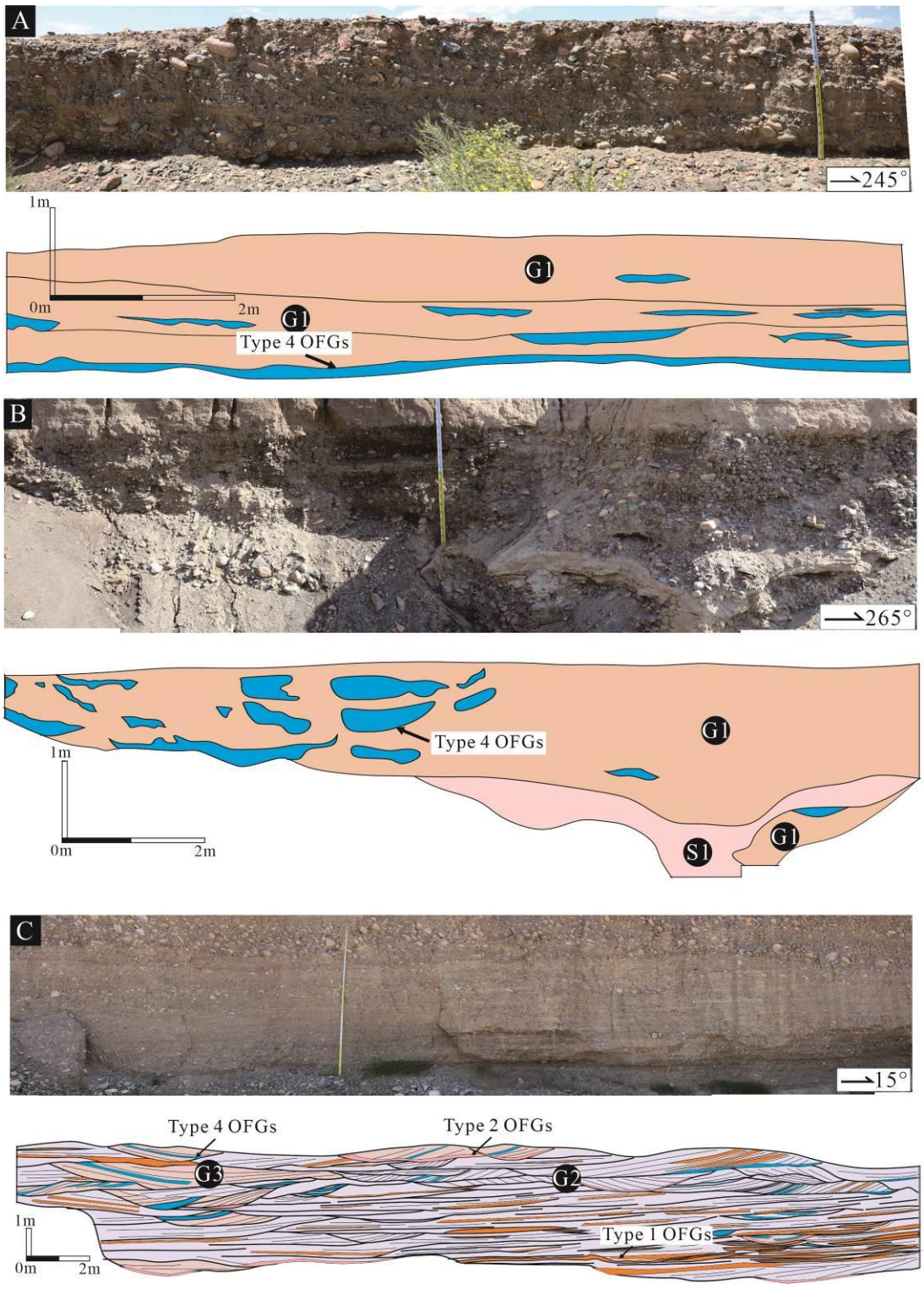

Fig.13 Photomosaics and architectural panels of the open-framework gravels in outcrop sections of the Poplar Fan. (A) Type 4 OFGs of channel origin. (B) Type 4 OFGs developed in sheet-like flow deposits of the proximal fan. (C) Type 1 and subordinate Type 2 and 4 OFGs from the medial fan. (D) OFGs of types 2 and 4 from the lower medial fan. (E) Type 3 OFGs from the distal fan. (F) Type 6 OFGs from the distal fan.

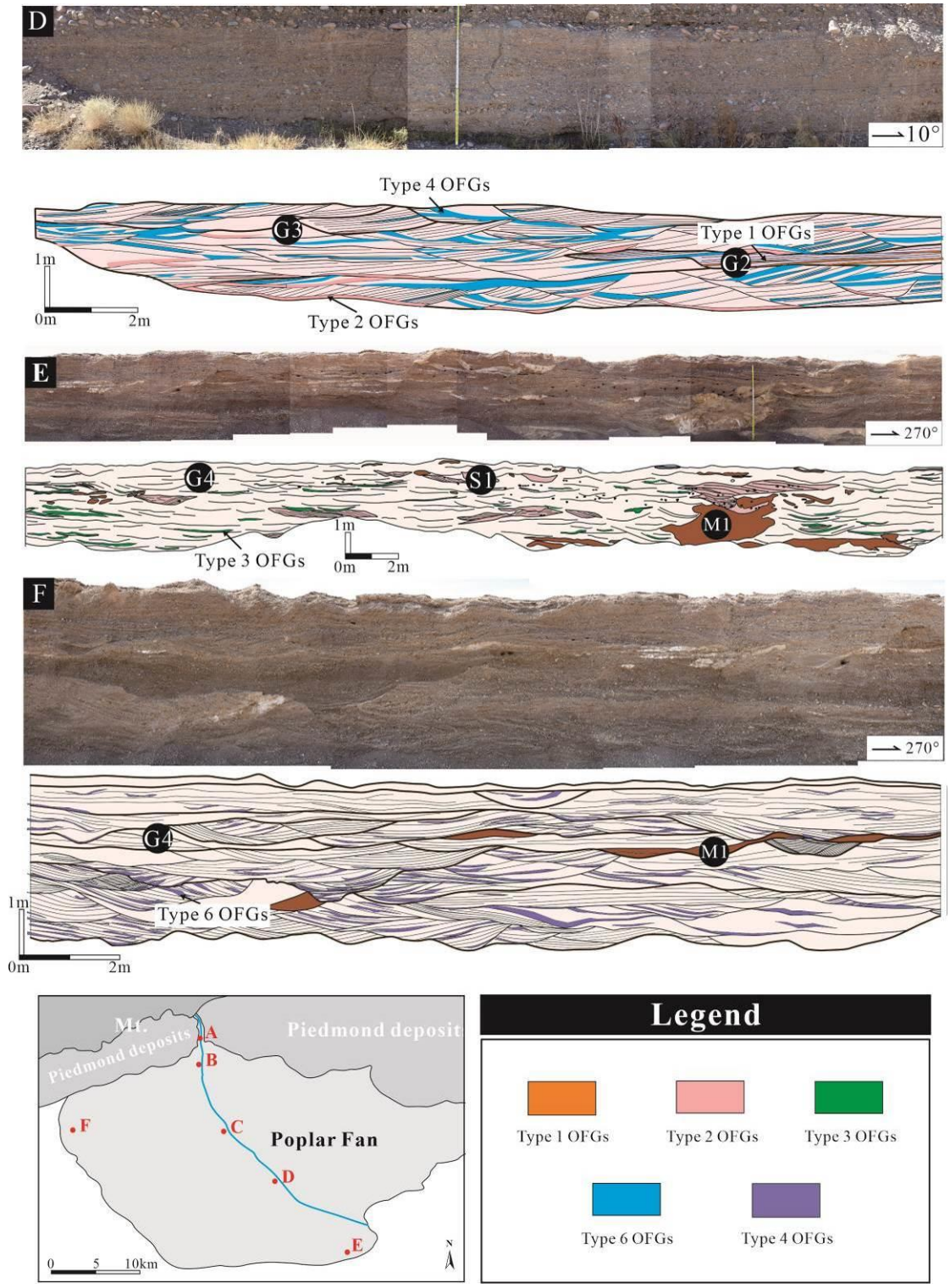

5. Discussion

5.1 Depositional model of open-framework gravels

In alluvial-fan settings, OFGs are dominantly observed in the deposits of sheetflood, debris-flow or channelized streamflow processes (e.g., Jo et al., 1997; Blair 2000;

Zappa et al., 2006; Milana, 2010; Colombera and Bersezio, 2011), which are variably associated with flood and interflood stages (cf. Gao, 2020). The temporal and spatial variability in the occurrence of these flow processes controls the types and spatial distribution of OFGs. Based on sedimentological observations and hydrological data from the Poplar Fan, a novel depositional model is proposed to account for the distribution of OFGs in similar alluvial-fan successions.

In the studied deposits, the principal genetic mechanism for the formation of OFGs is the process of sediment winnowing, whereby finer particles are entrained and removed by water or wind, leaving behind the coarser fraction (cf., Ramos and Sopeña, 1983; Siegenthaler and Huggenberger, 1993; Laronne and Shlomi 2007; Lunt and Bridge, 2007; Waters et al., 2010). This process appears to dominate across all types of OFGs, whether be they related to deposition associated with high or low flow stages.

The spatiotemporal distribution of different types of OFGs in the Poplar Fan (Fig. 14) can be summarized as follows. OFGs that were accumulated during the high flow stage are the most abundant in relative terms (Fig. 12). In the fan-head trench high-energy floods emanate from the catchment causing the deposition of massive gravels (G1) within the lateral confinement of the valley; here, OFG deposits are lacking (Blair, 1999; Alexander, 2001; Goswami, 2018). The overall unstratified lithofacies G1, with its poorly sorted and chaotic fabric, common presence of floating outsized boulders, and indistinct imbrications, is interpretable as the product of non-selective and partially en-masse deposition by hyperconcentrated flows (DeCelles et al., 1991; Blair and McPherson, 2009). At times and locations where stream floods are supercritical, Type 1 OFGs dominate in the proximal fan sector, where they exhibit a wide range of lateral extensions. The sheet-like flow deposits take the form of alternating coarse-fine planar couplets, in which the Type 1 OFGs are present in high proportion (from 4% to >20%). In particular, laterally extensive amalgamated gravel beds represent composite deposits resulting from the stacking of multiple lobes produced by formative supercritical sheet-like flows, which may have occurred as part of multiple flood events (cf. Blair and McPherson, 2009; North and Davidson, 2012; Antronico et al., 2015). In the medial fan sector, Type 2 OFGs with low-angle (5° to 10°) trough cross-stratification are interpreted as having dominantly accumulated under conditions of unconfined subcritical streamflows (Allen, 1981; North and Davidson, 2012; Chen et al., 2017), as commonly seen in modern piedmont river systems during floods (Abdullatif, 1989). Type 3 OFGs occur along the bed of narrow channels in the distal fan (Fig.16-A). They are less common at the fan fringe, due to

the limited activity of groundwater-fed flows. Type 1, 2 and 3 OFGs are the principal OFG types that originated during the high flow stage, and their spatial distribution reflects the distribution of areas subject to different types of high flow stage processes (Fig.4-A).

During the low flow stage, erosional and depositional processes on the fan surface are concentrated along a distributary channel network exhibiting braided, single-thread low-sinuosity, and meandering planforms (cf. Jolivet et al., 2015; Gao et al., 2018). The distribution of OFGs of low-flow-stage origin reflects the areas where braided channels were active, whose extent is markedly more limited than that of areas subject to the high flow stage. Type 4 OFGs tend to occur on the streambed of braided channels (cf. Guin et al., 2010), which are seen in the hosting channels of the proximal fan and in the sets of trough cross-bedding of the medial to distal fan. (Fig. 14-B). From the proximal fan to the fan fringe, the width, thickness and maximum particle size of units of Type 4 OFGs decreases gradually due to channel bifurcation. Type 5 OFGs occur in compound bar deposits, which are associated with the migration of unit bars with coarse bar heads (Lunt et al., 2004; Lunt and Bridge, 2007). They are most commonly observed near the tops and along the sides of the unit bars.

In inactive distal fan sectors, Type 6 OFGs occur at the base of gulleys. These OFGs developed during ephemeral surficial flows triggered by rainwater convergence (De Haas et al., 2015a). These ephemeral flows run over pre-existing river deposits that were originally deposited by flows of higher velocity and hydrodynamic power (Miall, 1996; Went, 2005), causing winnowing of their finer-grained particles. OFGs of types 7 and 8 are rare and only occur locally.

Across the fan as a whole, OFGs of types 1, 2 and 4 are most common. The OFGs of low flow stage have more distinctly defined bed boundaries, better sorting and greater clast roundness. Thus, OFG types of low flow stage origin may have higher values of porosity and permeability compared to those of high flow stage, due to the more prolonged winnowing action they might have experienced.

Among the alluvial systems, the formative processes and spatial distribution of OFGs have obvious differences. Based on the primary mode of sediment transport and deposition, alluvial fans can generally be categorized into debris-flow dominated fans (cf. Blair and McPherson, 2009; Harvey, 1999), and stream-flow dominated fans (cf. DeCelles et al., 1991; Colombera and Bersezio, 2011; Franke et al., 2015). Depending on the process regime of a fan, the formative processes, spatial distribution and characteristics of OFGs can vary considerably. The Poplar Fan is streamflow

dominated, and characteristically lacks OFGs associated with debris-flow deposition. In debris-flow fans, OFGs tend to notably accumulate in the frontal and top portions of non-cohesive debris-flow lobes (Johnson et al., 2012; De Haas et al., 2015b; Kim et al., 2021). In sheetflood-dominated alluvial fans, OFGs deposit can occur in planar-stratified couplets mantling the fan surface (Ballance, 1984; Blair, 1999). The formative processes of Type 1 OFGs are similar to those of sheetflood-dominated alluvial fans. Type 1 OFGs only accumulate at the proximal to medial fan region of the Poplar Fan. However, in sheetflood-dominated alluvial fans, the OFGs occur from apex to toe (Blair, 2000; Alexander et al., 2001; Kim et al., 2021). In streamflow-dominated alluvial fans, the formative processes and spatial distribution of OFGs are comparable to those observed for the deposits of low flow stage of the Poplar Fan. OFG deposits are seen to form lenticular bodies of trough cross-stratified units and gravel bodies with locally sigmoidal cross-stratification (Ori, 1982; Ramos and Sopeña, 1983; Siegenthaler and Huggenberger, 1993; Lunt and Bridge, 2007). On abandoned or inactive fan sectors, the alluvial-fan surface is reworked by precipitation-driven overland flows and wind during interflood periods. Thus, Type 6 and Type 8 OFGs may occur in most alluvial-fan systems (Blair, 2000; North and Davidson, 2012; Gao et al., 2020). Compared with other alluvial systems, the OFGs of the Poplar Fan display significant variability in origin, since their formative processes include sheet-like floods, channelized streamflows, overland flows and wind transport. As such, the Poplar Fan reveals particular complexity in the distribution of OFGs in the preserved fan architecture.

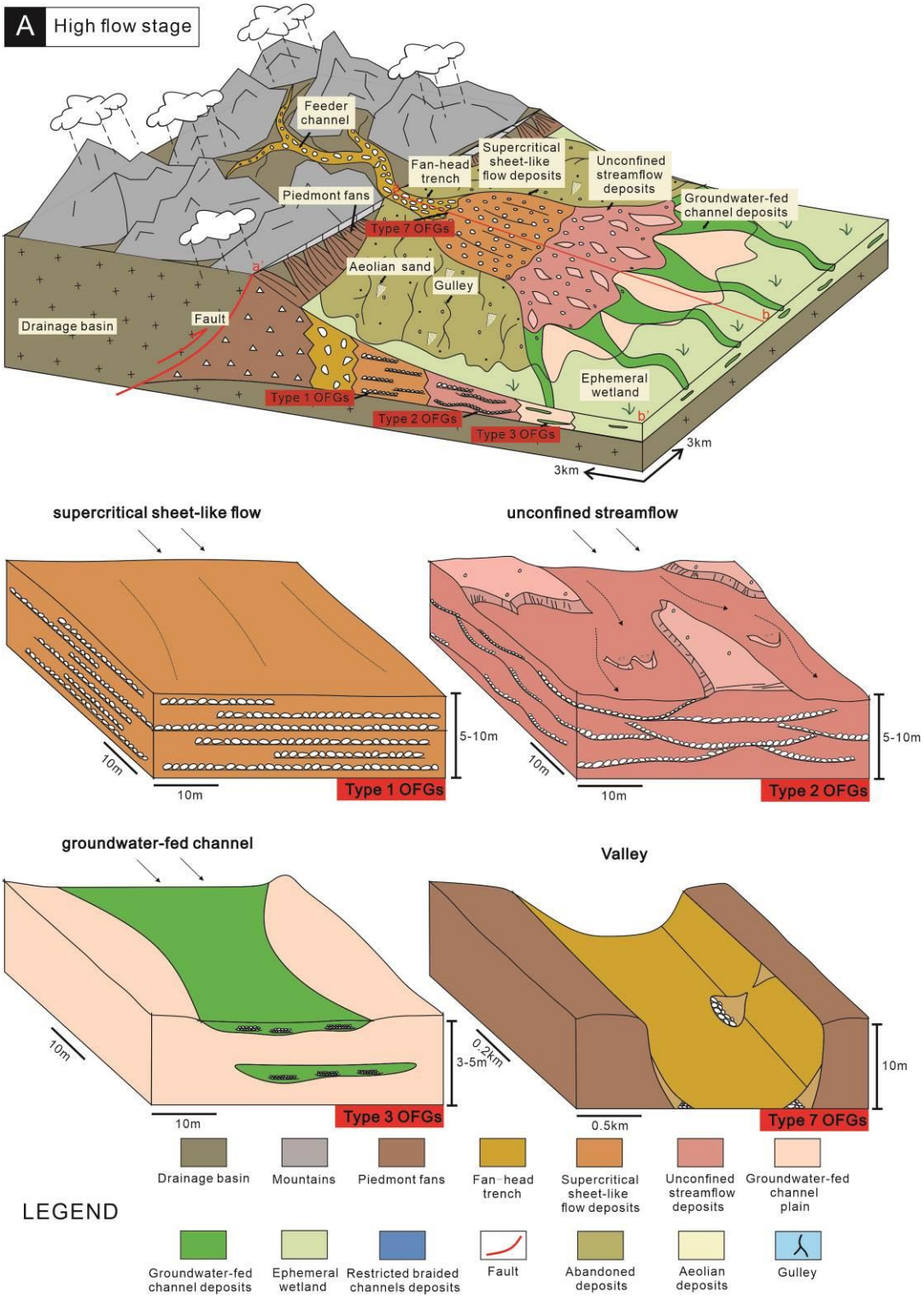
A High flow stage
Feeder channel
Fan-head trench
Supercritical sheet-like flow deposits
Unconfined streamflow deposits
Groundwater-fed channel deposits
Piedmont fans
Type 7 OFGs
Aeolian sand
Gulley
Drainage basin
Fault
Ephemeral wetland
Type 1 OFGs
Type 2 OFGs
Type 3 OFGs
3km
3km
supercritical sheet-like flow
unconfined streamflow
5-10m
10m
10m
Type 1 OFGs
5-10m
10m
10m
Type 2 OFGs
groundwater-fed channel
Valley
10m
3-5m
10m
Type 3 OFGs
0.2km
0.5km
10m
Type 7 OFGs
LEGEND
Drainage basin
Mountains
Piedmont fans
Fan-head trench
Supercritical sheet-like flow deposits
Unconfined streamflow deposits
Groundwater-fed channel plain
Groundwater-fed channel deposits
Ephemeral wetland
Restricted braided channels deposits
Fault
Abandoned deposits
Aeolian deposits
Gulley

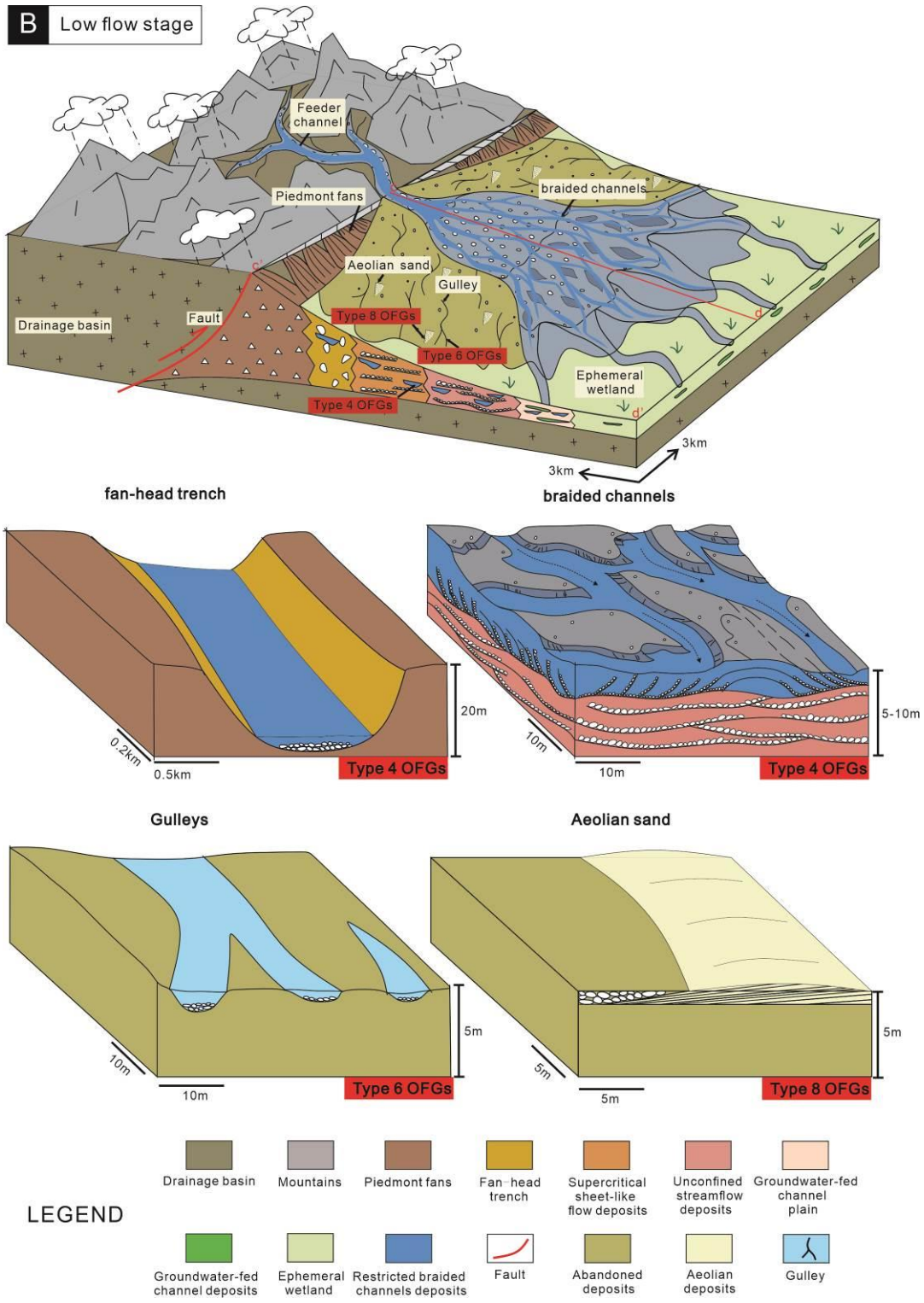

Fig.14 Schematic depositional model showing the distribution of open-framework gravels associated with the two stages of construction of the Poplar Fan, depicting their distribution across the fan and in related subenvironments. (A) Open-framework gravels associated with episodic high flow stages. (B) Open-framework gravels associated with low flow stages.

5.2 Implications for hydrocarbon-reservoir characterization

Alluvial-fan successions form hydrocarbon reservoirs of variable sizes in many petroliferous basins (e.g. Cook Bay in USA, Cuyo in Argentina, Sergipe-Alagoas in Brazil) (Elliott and Diver, 1971), and are especially important targets in the Mahu sag of the Junggar Basin in China, which contains the largest alluvial fan conglomerate oilfield in the world (Zhang et al., 1985; Wu et al., 2012). In this context, complex internal lithofacies heterogeneity and variability in primary reservoir quality are determined by a variety of sediment-transport processes. It is common for alluvial-fan successions to have limited reservoir quality, in view of their poor sorting; values of porosity and permeability are characteristically lower than those seen in the facies forming net intervals of fluvial reservoirs (Qiu, 1992; Moscariello, 2018). However, some alluvial-fan successions, notably including some in the Mahu sag of the Junggar Basin, have potential as hydrocarbon reservoirs. For these successions, it is paramount to predict the occurrence of favourable reservoir units that are potential targets for hydrocarbon exploration, and of permeability contrasts that may affect recovery rates.

Open-framework gravels commonly act as preferential-flow pathways; these define thief zones during water flooding or miscible gas injection in hydrocarbon reservoirs, or cause the rapid, localized dispersion of groundwater contaminants in aquifers (Klingbeil et al., 1999; Ronayne et al., 2010; Gershenzon et al., 2015b, c). This is because OFGs can have values of permeability that are three to four orders of magnitude greater than those of other associated alluvial deposits (Ferreira et al., 2010; Gershenzon et al., 2015c). During burial, poorly sorted deposits generally undergo a more rapid reduction in porosity via mechanical compaction, compared to better sorted deposits (Revil, 2002; Salem et al., 2005; Gao et al., 2020). In view of their original porosity and limited compaction, compared with other alluvial-fan lithofacies, OFGs tend to be more homogeneous and significantly better sorted. In some circumstances, OFGs can form the dominant reservoir units in alluvial-fan successions hosting oil and gas accumulations (Gong et al. 2019). This can be the case where the pores of OFGs are partially cemented, causing a significant reduction in their permeability while preserving some of the original porosity (Hay, 1966; Fu et al., 2010; Zhang et al., 2020a); under these conditions, it is notable that OFGs do not form thief zones, but rather constitute one of the principal targets of alluvial-fan reservoirs.

In these situations, the trends in OFG sedimentation recognized on the Poplar Fan can be applied to predict the distribution and geometry of favourable reservoir intervals of alluvial-fan successions. Predictions of this type are required, for example, for the lower Permian Wuerhe Formation (P2w) of the Junggar Basin, in which productive reservoir units that were originally formed as OFGs are recognized in coreholes (Fig.

15b). Close to the north-western margin of the Junggar Basin, the Wuerhe Formation is composed mostly of alluvial-fan deposits that were dominantly deposited by flash floods in an arid setting (Zhang et al., 2020a). Based on the identification of paraconformities and unconformities produced by extended periods of non-deposition or erosion, several depositional sequences are recognized across 16 cored boreholes with a cumulative core length of 275 m (Zhang et al., 2020a). Open-framework conglomerates with oil shows make up ca. 7% of the alluvial-fan successions (Fig.15a, b) which is comparable with the proportion seen for the Poplar Fan. Cored intervals consisting of disaggregated gravels are identified as open-framework conglomerates (Fig.15b). Part of the pore space of the open-framework conglomerates is cemented by zeolites, which have been partly dissolved by organic acids (Hay, 1966; Fu et al., 2010). As a result, open-framework conglomerates of the Wuerhe Formation have porosity of 7.0% to 25.5% and permeability of 50 to 945 mD. Identification and prediction of the occurrence of open-framework conglomerates in the subsurface rely heavily on the integration of data from wireline logs, borehole images and cores. In core, open-framework conglomerates of the Wuerhe Formation display clast imbrication and units have erosional bases. These deposits occur as part of sections interpreted as braided-channel deposits (Fig.15a, b) (cf. Zhang et al., 2020a; Gao et al; 2021). In thin section, the clast-supported and porous nature of the facies is evident (Fig.15c).

The distribution of OFGs documented in the streamflow-dominated Poplar Fan can be applied in contexts of subsurface characterization in the following ways: (i) it allows estimates of the likely spatial variability in the contribution of OFGs in the facies make-up of alluvial-fan successions; (ii) it enables interpretation of the depositional conditions and sub-environments of deposition of different types of open-framework conglomerates seen in preserved ancient alluvial-fan deposits; (iii) it provides constraints with which to ensure that realistic scaling and orientation of OFG units is incorporated in reservoir models and well correlations.

In the type 1 and 2 OFGs, due to the lack of internal heterogeneities that can act as flow baffles, no or little residual oil remains after primary development. However, in the type 4 and 5 OFGs, more residual oil may be present due to the occurrence of cross-bedding where the injection water cannot reach due to petrophysical heterogeneity determined by textural variations (alternation of volumes with occluded and openwork frameworks) that cause poorer sweep efficiency (Ma et al., 1999; Miall, 2014; Zhang et al., 2020b). The identification of a specific type of open-framework conglomerate may be rendered difficult where these are poorly cemented and tend to

disaggregate into loose clasts in core; in these cases, the possible origin of the OFGs can be suggested based on the characteristics of adjacent and genetically related deposits, and based on knowledge of trends in processes across fan sectors.

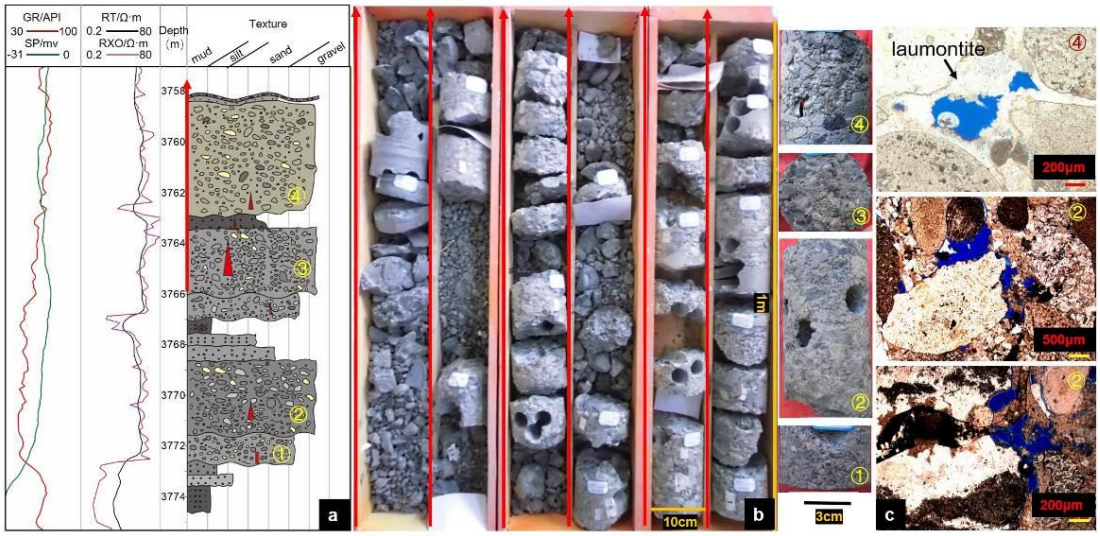

Fig.15 Well data from the lower Permian Wuerhe Formation (P2w). (a) Lithofacies characters in well logs. (b) Core sections containing disaggregated conglomerates. (c) Thin section of cemented openwork conglomerates.

6. Conclusions

Open-framework gravels are an important lithofacies in alluvial-fan successions; they are characterized by less than 15% of sand or fines. Owing to the notable scarcity of sand or mud, and to the well-sorted nature of the gravels, good pore connectivity and high permeability are typical features of these deposits.

Based on an understanding of the sedimentary processes that operate on the Poplar Fan (China), the distinct records of high and low flow stages can be identified. The OFG deposits can be classified into eight types that can be related to these two stages. In the high flow stage, OFGs associated with supercritical and subcritical unconfined flows and with groundwater-fed channels (types 1, 2 and 3) tend to develop according to a spatial trend, from the proximal fan to the fan fringe. Due to scour by sheet-like flows, these types of OFGs tend to occur at the bottom of deposits of waning floods. In the low flow stage, trough and sigmoidal cross-stratified OFGs (types 4 and 5) are associated with deposition on braided channels traversing the fan. OFGs associated with gulleys, wall collapse or aeolian activity (types 6, 7 and 8) occur on inactive fan lobes or along valley walls, throughout the fan.

The distribution of OFGs across the fan demonstrates some spatial trends. In the proximal fan, only Type 4 OFGs are seen, in channel subenvironments. In the medial fan, OFGs of types 4 and 5 occur interbedded with units containing types 1 and 2. At

the fan fringe, OFGs are largely seen as being of types 3 and 6. Across the entire fan, OFGs comprise ~7% of all deposits. OFG types 1, 2 and 4 are the most common.

This study provides a comprehensive quantitative summary characterization of how OFGs vary in origin and distribution in streamflow-dominated alluvial fans, in the form of a novel depositional model. This model can be applied to (i) guide further investigations on the origin and distribution of OFGs in complex alluvial-fan successions, and (ii) as a predictive template with which to account for lithological heterogeneity (porosity and permeability distribution) in the characterization of alluvial-fan successions of comparable origin, targeted for the production of oil, gas and water.

Acknowledgements

This study is financially supported by the National Natural Science Foundation of China (No. 42072115 and 41902118). We thank PetroChina Xinjiang Oilfield Company for their support in completing this research. LC and NPM thank the sponsors of the Fluvial, Eolian and Shallow-Marine Research Group (AkerBP, Areva (now Orano), BHPBilliton, Cairn India (Vedanta), Chevron, CNOOC International, ConocoPhillips, Equinor, Murphy Oil, Occidental, Saudi Aramco, Shell, Tullow Oil, Woodside and YPF) for financial support. Dr. Young Kwan Sohn is thanked for his comments, which have improved the article.

References

Abdullatif, O.M., 1989. Channel-fill and sheet-flood facies sequences in the ephemeral terminal River Gash, Kassala, Sudan. Sedimentary Geology 63, 171-184.

Ai, K.K., Ji, J.L., 2015. Tectonic uplift of mountains in Northwestern Junggar since Late Cenozoic: evidences from sedimentology and magnetic in Heshituoluogai Bain. Earth Science 40, 535-547 (in Chinese with English abstract).

Alexander, J., Bridge, J.S., Cheel, R.J., Leclair, S.F., 2001. Bedforms and associated sedimentary structures formed under supercritical water flows over aggrading sand beds. Sedimentology 48, 133-152.

Allan, A.F., Frostick, L., 1999. Framework dilation, winnowing, and matrix particle size; the behavior of some sand-gravel mixtures in a laboratory flume. Journal of Sedimentary Research 69, 21-26.

Allen, J.R.L. 1983a. Studies in fluviatile sedimentation: Bars, bar-complexes and sandstones sheet (low-sinuosity streams) in the Brownstones (L. Devonian), Welsh Borders. Sedimentary Geology 33, 237-293.

Allen, J.R.L. 1983b. Gravel overpassing on humpback bars supplied with mixed sediment: examples from the Lower Old Red Sandstone, southern Britain. Sedimentology 30, 285-294.

Allen, P.A., 1981. Sediments and processes on a small stream-flow dominated, devonian alluvial fan, Shetland Islands. Sedimentary Geology 29, 31-66.

Al-Farraj, A., Harvey, A.M., 2000. Desert pavement characteristics on wadi terrace and alluvial fan surfaces, Wadi Al-Bih, UAE and Oman. Geomorphology 35, 279-297.

Antronico, L., Greco, R., Robustelli, G., Sorriso-Valvo, M., 2015. Short-term evolution of an active basin-fan system, Aspromonte, south Italy. Geomorphology 228, 536-551.

Ballance, P.F., 1984. Sheet-flow-dominated gravel fans of the nonmarine middle Cenozoic Simmler Formation, central California. Sedimentary Geology 38, 337-359.

Banham, S.G., Mountney, N.P., 2013. Controls on fluvial sedimentary architecture and sediment-fill state in salt-walled mini-basins: Triassic Moenkopi Formation, Salt Anticline Region, SE Utah, USA. Basin Research 25, 709-737.

Blair, T.C., 1999. Sedimentary processes and facies of the water-laid Anvil Spring Canyon alluvial fan, Death Valley, California. Sedimentology 46, 913-940.

Blair, T.C., 2000. Sedimentology and progressive tectonic unconformities of the sheet flood dominated Hell's Gate alluvial fan, Death Valley, California. Sedimentary Geology 132, 233-262.

Blair, T.C., McPherson, J.G., 2009. Processes and forms of alluvial fans. In: Parsons, A.J., Abrahams, A.D. (Eds.), Geomorphology of Desert Environments, 2nd ed. Springer, Netherlands, pp. 413-467.

Blissenbach, E., 1954. Geology of alluvial fans in semiarid regions. Bulletin of the Geological Society of America 65, 175-190.

Blott, J.S., Pye, K., 2001. Gradistat: A grain size distribution and statistics package for the analysis of unconsolidated sediments. Earth Surface Processes and Landforms 26, 1237-1248.

Braden, G.E., 1955. Openwork gravel deposits in stream valleys. Proceedings of the Oklahoma Academy of Science 36, 88-89.

Burbery, L.F., Moore, C.R., Jones, M.A., Abraham, P.M., Humphries, B.L., Close, M.E., 2017. Study of connectivity of open framework gravel facies in the Canterbury Plains aquifer using smoke as a tracer. Geological Society, vol. 440. London, Special Publication, 327-344.

Cain, S.A., Mountney, N.P. 2009. Spatial and temporal evolution of a terminal fluvial fan system: the Permian Organ Rock Formation, South-east Utah, USA. Sedimentology 56, 1774-1800.

Cao, Y.C., Yang, T., Wang, Y.Z, Li, W.Q., 2017. Formation, evolution and sedimentary characteristics of supercritical sediment gravity-flow. Acta Petrolei Sinica 38, 607-621 (in Chinese with English abstract).

Cartigny, M.J.B., Ventra, D., Postma, G., Van, D.B., Jan, H., Venditti, J., 2014. Morphodynamics

and sedimentary structures of bedforms under supercritical-flow conditions, New insights from flume experiments. Sedimentology 61, 712-748.

Chen, L., Steel, R.J., Guo, F., Olariu, C., Gong, C.L., 2017. Alluvial fan facies of the Yongchong Basin, Implications for tectonic and paleoclimatic changes during Late Cretaceous in SE China. Journal of Asian Earth Sciences 134, 37-54.

Chou, H.T., Lee, C.F., Lo, C.M., 2017. The formation and evolution of a coastal alluvial fan in eastern Taiwan caused by rainfall-induced landslides. Landslides 14, 109-122.

Clarke, L., Quine, T.A., Nicholas, A., 2010. An experimental investigation of autogenic behaviour during alluvial fan evolution. Geomorphology 115, 278-285.

Clarke, L., 2015. Experimental alluvial fans, Advances in understanding of fan dynamics and processes. Geomorphology 244, 135-145.

Colombera, L., Bersezio, R., 2011. Impact of the magnitude and frequency of debris-flow events on the evolution of an alpine alluvial fan during the last two centuries: responses to natural and anthropogenic controls. Earth Surface Processes and Landforms 36, 1632-1646.

Colombera, L., Mountney, N.P., 2019. The lithofacies organization of fluvial channel deposits: a meta-analysis of modern rivers. Sedimentary Geology 383, 16-40.

Cuevas Gozalo, M.C., Martinius, A.W., 1993. Outcrop data-base for the geological characterization of fluvial reservoirs: an example from distal fluvial fan deposits in the Loranca Basin, Spain. In: North, C.P., Prosser, D.J. (Eds.), Characterisation of Fluvial and Aeolian Reservoirs., Geological Society, vol. 73. London, Special Publication, pp. 79-94.

DeCelles, P.G., Gray, M.B., Ridgway, K.D., Cole, RB., Pivnik, D.A., Pequera, N., Srivastava, P., 1991. Controls on synorogenic alluvial-fan architecture, Beartooth gravels (Palaeocene), Wyoming and Montana. Sedimentology 38, 567-590.

De Haas, T., Kleinhans, M.G., Carbonneau, P.E., Rubensdotter, L., Hauber, E., 2015a. Surface morphology of fans in the high-Arctic periglacial environment of Svalbard, Controls and processes. Earth-Science Reviews 146, 163-182.

De Haas, T., Braat, L., Jasper, R.F.W., Leuven, Lokhorst, I.R., Kleinhans, M.G., 2015b. Effects of debris flow composition on runout, depositional mechanisms and deposit morphology in laboratory experiments. Journal of Geophysical Research (Earth Surface) 120, 1949-1972.

Doeglas, D.T., 1968. Grain-size indices, classifications and environment. Sedimentology 10, 83-100.

Du, G.Y., Lv, H.H., Wang, G.C., Ji, J.L., Zhang, L., Wu, Y., Xu, B., Xie, J.H., 2013. The division of four levels of planation surfaces and the partition of tectonic geomorphology in West Junggar Mountain. Earth Science Frontiers, 20, 256-262 (in Chinese with English abstract).

Elliott, W.H., Diver, C.J., 1971. Early Reservoir Modeling of Trading Bay unit Hemlock Formation. SPE 3243.

Eriksson, K.A., Vos, R.G., 1979. A fluvial fan depositional model for middle Proterozoic red beds from the Waterberg Group, South Africa. Precambrian Research 372, 169-188.

Ferreira, J.T., Jr, R.W.R., Dominic, R., 2010. Measuring the permeability of open-framework gravel. Groundwater 48, 593-597.

Fisher, J.A., Waltham, D., Nichols, G.J., Krapf, C.B.E., Lang, S.C., 2007. A quantitative model for deposition of thin fluvial sand sheets. Journal of the Geological Society 164, 67-71.

Folk, R.L., 1966. A review of grain-size parameters. Sedimentology 6, 73-93.

Franke, D., Hornung, J., Hinderer, M., 2015. A combined study of radar facies, lithofacies and three-dimensional architecture of an alpine alluvial fan (Illgraben fan, Switzerland). Sedimentology 62, 57-86.

Fu, G.M., Dong, M.C., Zhang, Z.S., Sun, L., Pan, R., 2010. Formation process and distribution of laumontite in Yanchang 3 reservoir of Fuxian exploration area in North Shaanxi province and the controls of the high quality reservoirs. Earth Science - Journal of China University of Geosciences 35: 107-114 (in Chinese with English abstract).

Gao, C.L., Ji, Y.L., Wu, C.L., Jin, J., Ren, Y., Yang, Z., Liu, D.W., Huan, Z.J., Duan, X.B., Zhou, Y.Q., 2020. Facies and depositional model of alluvial fan dominated by episodic flood events in arid conditions, An example from the Quaternary Poplar Fan, north-western China. Sedimentology 67, 1750-1796.

Gao, C.L., Ren, Y., Wang, J., Ji, Y.L., Liu, B., Xiong, L.Q., Sun, Y.H., Wang, K., Liu, K., 2021. Palaeohydraulic reconstruction and depositional model of the episodic flooding channels developed in the modern arid alluvial fan: Implications for the exploration target of the heterogeneous alluvial fan reservoirs. Journal of Petroleum Science and Engineering 205, 108927.

Gao, L., Wang, X., Yi, S., Vandenberghe, J., Gibling, M., Lu, H., 2018. Episodic sedimentary evolution of an alluvial fan (Huangshui Catchment, NE Tibetan Plateau). Quaternary 1, 16.

Cary, A.S. 1951. Origin and Significance of Openwork Gravel. Transactions of the American Society of Civil Engineers 116, 1296-1318.

Gershenzon, N.I., Ritzi, R.W., Dominic, D.F., Soltanian, M., Mehnert, E., Okwen, R.T., 2015a. Influence of small-scale fluvial architecture on CO_2 trapping processes in deep brine reservoirs. Water Resources Research 51, 8240-8256.

Gershenzon, N.I., Soltanian, M.R., Ritzi, R.W., Jr., Dominic, D.F., Keefer, D., Shaffer, E., Storsved, B., 2015b. How does the connectivity of open-framework conglomerates within multi-scale hierarchical fluvial architecture affect oil-sweep efficiency in waterflooding? Geosphere 11, 2049-2066.

Gershenzon, N.I., Soltanian, M., Ritzi, R.W., Dominic, D.F., 2015c. Understanding the impact of open-framework conglomerates on water-oil displacements: the Victor interval of the Ivishak

Reservoir, Prudhoe Bay Field, Alaska. Petroleum Geoscience 21, 43-54.

Glaister, R.P., and Nelson, H.W., 1974. Grain-size distributions, an aid in facies identification. Bulletin of Canadian Petroleum Geology 22, 203-240.

Gong, Q.S., Liu, Z.G., Pang, X., Li, L.M., Xie, L., Zhu, C., 2019. Heterogeneity of sandy gravels reservoir and its influence on remaining oil distribution: A case study of Qie 12 block of Kunbei oilfield in Qaidam basin. Journal of China University of Mining and Technology 48, 165-174.

Goswami, P.K., Kshetrimayum, A.S., 2018. Depositional processes and sedimentation pattern in an intermontane basin, Insights from the Imphal Basin, Indo-Myanmar Range, NE India. Geological Journal 53, 1-13.

Guin, A., Ramanathan, R., Ritzi, R.W., Dominic, D.F., Lunt, I. A., Scheibe, T.D., Freedman V.L. 2010. Simulating the heterogeneity in braided channel belt deposits: 2. examples of results and comparison to natural deposits. Water Resources Research 46, 292-305.

Guha, A., Roy, P., Singh, S., Vinod, K., 2018. Integrated use of LANDSAT 8, ALOS-PALSAR, SRTM DEM and ground GPR data in delineating different segments of alluvial fan system in Mahananda and Tista Rivers, West Bengal, India. Journal of the Indian Society of Remote Sensing 46, 501-514.

Guo, J.H., 2003. Wet alluvial fan sedimentary in the Guantao formation of Shuyi area. Acta Sedimentologica Sinica 21, 367-371.

Hay, R.L., 1966. Zeolites and zeolitic reactions in sedimentary rocks. Geological Society of America Special Papers 85, 1-122.

Hooke, R. L., 1967. Processes on arid-region alluvial fans. Journal of Geology 75, 438-460.

Harvey, A.M., Silva, P.G., Mather, A.E., Goy, J.L., Stokes, M., Zazo, C., 1999. The impact of Quaternary sea-level and climatic change on coastal alluvial fans in the Cabo de Gata ranges, southeast Spain. Geomorphology 28, 1-22.

Hornung, J., Pflanz, D., Hechler, A., Beer, A., Hinderer, M., Maisch, M., Bieg, U., 2010. 3-D architecture, depositional patterns and climate triggered sediment fluxes of an alpine alluvial fan (Samedan, Switzerland). Geomorphology 115, 202-214.

Hürlimann, M, Rickenmann, D., Graf, C., 2003. Field and monitoring data of debris-flow events in the Swiss Alps. Canadian Geotechnical Journal 40, 161-175.

Jo, H.R., Rhee, C.W., Chough, S.K., 1997. Distinctive characteristics of a streamflow-dominated alluvial fan deposit, Sanghori area, Kyongsang Basin (Early Cretaceous), southeastern Korea. Sedimentary Geology 110, 51-79.

Johnson, C.G., Kokelaar, B.P., Iverson, R.M., Logan, M., LaHusen, R.G., 2012. Grain-size segregation and levee formation in geophysical mass flows. Journal of Geophysical Research 117, F01032.

Jolivet, M., Bourquin, S., Heilbronn, G., Robin, C., Barrier, L., Dabard, M.P., Jia, Y., De Pelsmaeker, E., Fu, B., 2015. The Upper Jurassic-Lower Cretaceous alluvial-fan deposits of the Kalaza Formation (Central Asia): tectonic pulse or increased aridity? In: Brunet, M.F., McCann, T., Sobel, E.R. (Eds.), Geological Evolution of Central Asian Basins and the Western Tien Shan Range. Geological Society, vol. 427. London, Special Publication, pp. 491-521.

Kang, X., Hu W.X., Wang J., Cao, J., Yang, Z., 2017. Fandelta sandy conglomerate reservoir sensitivity: A case study of the Baikouquan formation in The Mahu sag, Junggar basin. Journal of China University of Mining and Technology 46, 576-585.

Kim, J., Woo, K.S., Lee, K.C., Sohn, Y.K., 2021. Overnight formation of a bouldery alluvial fan by a torrential rain in a granitic mountain (Mt. Seoraksan, Republic of Korea). The Sedimentary Record 19, 5-11.

Klingbeil, R., Kleineidam, S., Asprion, U, Aigner, T., Teutsch, G., 1999. Relating lithofacies to hydrofacies: outcrop-based hydrogeological characterisation of quaternary gravel deposits. Sedimentary Geology 129, 299-310.

Laronne, J.B., Shlomi, Y., 2007. Depositional character and preservation potential of coarse-grained sediments deposited by flood events in hyper-arid braided channels in the Rift Valley, Arava, Israel. Sedimentary Geology 19, 21-37.

Lee, H., Paik, I.S., Kim, H.J., Kang, H.C., Seol, W.G., Lee, J.Y., 2018. A discontinuity in the late Pleistocene alluvial deposits, Hwacheon-ri, Gyeongju, Korea, Occurrences and paleoenvironmental implication. Island Arc 27, 1-12.

Li, X.H., 2008. Hydrogeologic characteristic and prospect of uranium metallogenesis in Heshituoluogai Basin. Xinjiang Geology 26, 180-183 (in Chinese with English abstract).

Lin, R.F., Wei, K.Q., Cheng, Z.Y., Wang, Z.X., Gasse, F., Fontes, J.C., Gibert, E., Tucholka, P. 1996. A palaeoclimatic study on lacustrine cores from Manas Lake, Xinjiang, Western China. Geochimica 25, 63-71 (in Chinese with English abstract).

Liu, B., Tan, C., Yu, X., Yu, X.H., Qu, J.H., Zhao, X.M., Zhang, L., 2018. Sedimentary characteristics and controls of a retreating, coarse-grained fan-delta system in the Lower Triassic, Mahu depression, northwestern China. Geological Journal 54, 1-19.

Lunt, I.A., Bridge, J.S., Tye, R.S., 2004. A quantitative, three dimensional depositional model of gravelly braided rivers. Sedimentology 51, 377-414.

Lunt, I. A., Bridge, J. S., 2007. Formation and preservation of open-framework gravel strata in unidirectional flows. Sedimentology 54, 71-87.

Ma, S., Zhang, J., Jin, N., Wang, Z. Wang, Y., 1999. The 3D Architecture of Point Bar and The Forming and Distribution of Remnant oil. SPE Asia Pacific Improved Oil Recovery, SPE 57308.

Ma, D., He, D., Li, D., Tang, J., Liu, Z., 2015. Kinematics of syn-tectonic unconformities and implications for the tectonic evolution of the Hala'alat Mountains at the northwestern margin of the Junggar Basin, Central Asian Orogenic Belt. Geoscience Frontiers 6, 247-264.

Major, J.J., 1997. Depositional processes in large-scale debris-flow experiments. The journal of Geology 105, 345-366.

Malatesta, L.C., Berger, Q., Avouac, J.P., 2017. A model to quantify sediment mixing across alluvial piedmonts with cycles of aggradation and incision. Vienna, EGU General Assembly 2017. EGU General Assembly Conference Abstracts 10855.

McManus, J., 1988. Grain size determination and interpretation. Techniques in Sedimentology. Oxford, UK, Wiley Blackwell, 63-65.

Miall, A.D., 1977. A review of the braided river depositional environment. Earth Science Reviews 13, 1-62.

Miall, A.D., 1996. The Geology of Fluvial Deposits: Sedimentary Facies, Basin Analysis and Petroleum Geology. Springer Verlag, Berlin, 582 pp.

Miall, A.D., 2014. Fluvial depositional systems. Berlin, Springer, 2014, 24.

Milana, J.P., 2010. The sieve lobe paradigm: Observations of active deposition. Geology 38, 207-210.

Moscariello, A., 2018. Alluvial fans and fluvial fans at the margins of continental sedimentary basins: geomorphic and sedimentological distinction for geo-energy exploration and development. In: Ventra, D., Clarke, L.E. (eds.) Geology and geomorphology of alluvial and fluvial fans: current progress and research perspectives. Geological Society, London, Special Publications 440, 215-243.

Mountney, N.P. 2012. A stratigraphic model to account for complexity in aeolian dune and interdune successions. Sedimentology 59, 964-989.

North, C.P., Warwick, G.L., 2007. Fluvial fans: myths, misconceptions, and the end of the terminal-fan model. Journal of Sedimentary Research 77, 693-701.

North, C.P., Davidson, S.K., 2012. Unconfined alluvial flow processes: Recognition and interpretation of their deposits, and the significance for paleogeographic reconstruction. Earth-Science Reviews, 111, 199-223.

Novak, A., Popit, T., Šmuc, A., 2018. Sedimentological and geomorphological characteristics of Quaternary deposits in the Planica-Tamar Valley in the Julian Alps (NW Slovenia). Journal of Maps 14, 382-391.

Ori, G.G., 1982. Braided to meandering channel patterns in humid-region alluvial fan deposits, river reno, po plain (northern Italy). Sedimentary Geology 31, 231-248.

Passega, R., 1957. Texture as characteristic of elastic deposition: Am. Assoc. Petroleum Geologists Bull 41, 1952-1984.

Passega, R., 1964. Grain size representation by CM patterns as a geological tool. Journal of Sedimentary Research 34, 830-847.

Parsons, J.D., Whipple, K.X., Simoni, A., 2001. Experimental study of the grain-flow, fluid-mud transition in debris flows. The Journal of Geology 109, 427-447.

Pierson, T.C., Scott, K.M., 1985. Downstream dilution of a lahar: Transition from debris flow to hyperconcentrated streamflow. Water Resources Research 21, 1511-1524.

Prekopová, M., Janočko, J., Budinský, V., Friedmannová., M., 2016. Integration of seismic and sedimentological methods for analysis of Quaternary alluvial depositional systems. Environmental Earth Sciences 76, 25.

Pullen, A., Kapp, P., Chen, N.H., 2018. Development of stratigraphically controlled, eolian modified unconsolidated gravel surfaces and yardang fields in the wind-eroded Hami Basin, northwestern China. The Geological Society of America Bulletin 130, 630-648.

Qiu, Y.N., 1992. Developments in reservoir sedimentology of continental clastic rocks in China. Acta Sedimentologica Sinica 10, 16-24 (in Chinese with English abstract).

Qu, H.J., Hu, J.M., Li, W., Gao, S.L., Zhang, Y.L., Liu, J., Cui, J.J., 2008. The characteristics of sedimentation and tectonic evolution of Heishituoluogai Basin in Early Mesozoic, northwest Xinjiang. Acta Geologica Sinica 82, 441-450 (in Chinese with English abstract).

Ramos A., Sopeña A., 1983. Gravel bars in low-sinuosity streams (Permian and Triassic, central Spain). In: J.D. Collinson, J. Lewin (Eds.), Modern and Ancient Fluvial Systems. The International Association of Sedimentologists. vol. 6. Special Publication, pp. 301-312.

Ran, L., Zhu, H.J., Ziyabieke, A. 2010. Impact of climate change on hydrological regime in the Poplarhe river basin in Tacheng, Xinjiang during 1962-2007. Journal of Glaciology and Geocryology 32, 921-926 (in Chinese with English abstract).

Reid, I., Frostick, L.E., 1987. Towards a better understanding of bedload transport. In: Recent Development in Fluvial Sedimentology. In: F.G. Ethridge, R.M. Flores, M.D. Harvey. (Eds.), Society of Economic Paleontologists and Mineralogists. vol. 39. Special Publication, pp. 13-20.

Revil, A., 2002. Mechanical compaction of sand/clay mixtures. Journal of Geophysical Research 107, 2293.

Rhodes, T.E., Gasse, F., Lin, R.F., Fontes, J.C., Wei, K.Q., Bertrand, P., Gibert, E., Melieres, F., Tucholka, P., Wang, Z.X. Cheng, Z.Y., 1996. A Late Pleistocene-Holocene lacustrine record from Lake Manas, Zunggar (northern Xinjiang, western China). Palaeogeography, Palaeoclimatology, Palaeoecology 120, 105-121.

Ronayne, M.J., Gorelick, S.M., Zheng, C., 2010. Geological modelling of submeter scale heterogeneity and its influence on tracer transport in a fluvial aquifer. Water Resources Research 46, W10519.

Sahu, B.K., 1964. Depositional mechanisms from the size analysis of clastic sediments. Journal of Sedimentary Petrology 34, 73-83.

Salem, A.M., Ketzer, J.M., Morad, S., Rizk, R.R., Al-Aasm, I.S., 2005. Diagenesis and reservoir-quality evolution of incised-valley sandstones: evidence from the Abu Madi gas reservoirs (Upper Miocene), the Nile delta basin, Egypt. Journal of Sedimentary Research 75, 572-584.

Siegenthaler, C., Huggenberger, P., 1993. Pleistocene Rhine gravel: deposits of a braided river system with dominant pool preservation. In: Best, J. L. and Bristow, C. S. (Eds). Braided Rivers. Geological Society, vol.75. London, Special Publication, 147-162.

Shen, P., Pan, H., Shen, Y., Yan, Y. and Zhong, S., 2015. Main deposit styles and associated tectonics of the West Junggar region, NW China. Geoscience Frontiers 6, 175-190.

Shukla, U.K., 2009. Sedimentation model of gravel-dominated alluvial piedmont fan, Ganga Plain, India. International Journal of Earth Sciences 98, 443-459.

Steel, R.J., Thompson, D.B., 1983. Structures and textures in Triassic braided stream gravelss ('Bunter' Pebble Beds) in the Sherwood sands Group, North Staffordshire, England. Sedimentology 30, 341-367.

Sun, Z.M., 2015. Tectonic evolution, strike-slip and thrust reformation of Hoxtolgay Basin in Northwestern Xinjiang, China. Northwestern Geology 48, 150-158 (in Chinese with English abstract).

Tan, C.P., Yu X.H., Liu B.B., Xu, L., Li, S.L., Feng, S.Q., Tang, Y.S., 2018. Sedimentary structures formed under upper-flow-regime in seasonal river system: A case study of Bantanzi River, Daihai Lake, Inner Mongolia. Journal of Palaeogeography 2, 929-940.

Trendell, A. M., Atchley, S.C., Nordt, L.C., 2013. Facies analysis of a probable large-fluvial-fan depositional system, the Upper Triassic Chinle Formation at Petrified Forest National Park, Arizona, U.S.A. Journal of Sedimentary Research 83, 873-895.

Ventra, D., Clarke, L.E., 2018, Geology and geomorphology of alluvial and fluvial fans: Current progress and research perspectives. Ventra, D., Clarke, L.E. (Eds.), Geology and Geomorphology of Alluvial and Fluvial Fans: Terrestrial and Planetary Perspectives: Geological Society, vol. 440. London, Special Publication, pp.1-21.

Visher, G.S., 1965. Use of vertical profile in environmental reconstruction. AAPG Bull 49, 41-61.

Visher, G.S., 1969. Grain size distributions and depositional processes. Journal of Sedimentary Research 39, 1074-1106.

Wang, Y., Zhong, J.H., Wang, Z.K., Duan, H.L., Lian C.B., 2007. Sedimentary characteristics of modern alluvial fans in the northwest margin of the Qaidam Basin and their significance in petroleum geology. Geological Review 53, 791-796.

Waters, J.V., Jones, S.J., Armstrong, H.A., 2010. Climatic controls on late Pleistocene alluvial fans,

Cyprus. Geomorphology 115, 228-251.

Went, D.J., 2005. Pre-vegetation alluvial fan facies and processes: an example from the Cambro-Ordovician Rozel Conglomerate Formation, Jersey, Channel Islands. Sedimentology 52, 693-713.

Wu, S.H., Fan, Z., Xu. C.F., Yue, D.L., Zheng, Z., Peng, S.C., Wang, W., 2012. Internal architecture of alluvial fan in the Triassic Lower Karamay formation in Karamay oilfield, Xinjiang. Journal of Palaeogeography 14, 331-340.

Xu, A.N., Mu, L.X., Qiu, Y.N., 1998. Distribution pattern of OOIP and remaining mobile oil in different types of sedimentary reservoir of China. Petroleum Exploration and Development 25, 41-44.

Yu, S.Y., Du, J., Hou, Z., Shen, J., Colman, S.M., 2018. Late-Quaternary dynamics and palaeoclimatic implications of an alluvial fan-lake system on the southern Alxa Plateau, NW China. Geomorphology 327, 1-13.

Zappa, G., Bersezio, R., Fe Lletti, F., Giudici, M., 2006. Modeling heterogeneity of gravel-sand, braided stream, alluvial aquifers at the facies scale. Journal of Hydrology 325, 134-153.

Zhao, Y., Yu, Z.C. Chen, F.H. 2009. Spatial and temporal patterns of Holocene vegetation and climate changes in arid and semi-arid China. Quaternary. International 194, 6-18.

Zhang, J.Y. 1985. Some depositional characteristics and microfacies subdivision of coarse clastic alluvial fans. Acta Sedimentologica Sinica 3, 75-85.

Zhang, C.M., Song, X.M. Wang, X.J., Wang, X.L., Zhao, K., Shuang, Q., Li, S.H. 2020. Origin and depositional characteristics of supported conglomerates. Petroleum exploration and development 47, 292-305.

Zhang, Y., Ji Y.L., Gao, C. L., Jin, J., Yang, Z., Song, W.D., Bai, D.L., Liu, D.W., 2020a. Genetic mechanism, distribution and hydrocarbon geological significance of framework support gravels in Alluvial Fans. Journal of China University of Mining and Technology 49, 352-366.

Zhang, Y., Ji, Y.L., Wen, H.J., Ma, S.Z., Xing, B.K. 2020b. Flow unit model of channel sand body and its effect on remnant oil distribution: a case study of pi formation in the eastern transition zone of daqing oilfield. Geofluids 2020, 1-20.